In the present study, we report for the first time that the intermittent administration of methamphetamine increases the mRNA level of a C-C chemokine, CCR2, with histone modification in the limbic forebrain including the nucleus accumbens. To address the functional relevance of this increased CCR2 expression, we also investigated whether the increased locomotion observed after the intermittent administration of methamphetamine could be affected in CCR2 knockout mice.

The locomotor activity of mice was measured by an ambulometer (ANB-M20, O'Hara, Tokyo, Japan) as described previously. Briefly, male C57BL/6J mice or CCR2 knockout mice were obtained from Jackson Laboratories (Bar Harbor, ME, USA) and individually placed in a tilting-type round activity cage. To induce behavioral sensitization to methamphetamine-induced hyperlocomotion, the mice were given five intermittent treatments with methamphetamine (2 mg/kg, s.c.), once every 96 hours. To clarify the maintenance of behavioral sensitization, the mice were again administered methamphetamine (2 mg/kg, s.c.) after seven weeks of withdrawal.

The limbic forebrain area, mainly including the nucleus accumbens, was removed 24 hours after the last injection of methamphetamine. RNA preparation and semiquantitative analysis by reverse transcription polymerase chain reaction (RT-PCR) were performed as described previously. The methods are described in detail in the Supporting Information. The primers used are listed in Table S1.

Chromatin immunoprecipitation (ChIP) was performed as described previously with minor modifications. Soluble chromatin extracted from the mouse limbic forebrain was incubated with specific antibodies against acetylated histone H3 (Millipore; Billerica, MA, USA), H3K4 trimethylation (Wako Pure Chemicals, Osaka, Japan), H3K9 trimethylation (Millipore) and H3K27 trimethylation (Millipore) overnight at 4°C. The immunocomplex was collected by Dynabeads Protein A (Invitrogen Dynal AS, Oslo, Norway), and DNA was recovered by isopropanol precipitation. The methods are described in detail in the Supporting Information. The statistical analysis is also described in detail in the Supporting Information.

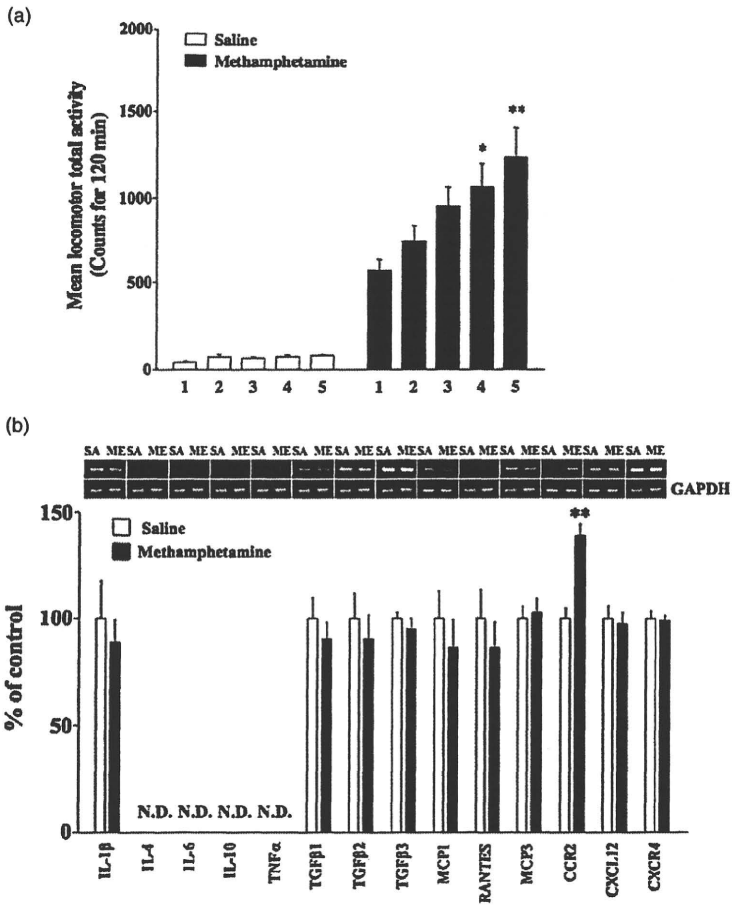

Figure 1 (a) Development of sensitization to methamphetamine in mice. Methamphetamine (2 mg/kg, s.c.) or saline was repeatedly given five times to mice every 96 hours. Total activity was counted for 120 minutes after each injection. Each column represents the mean total counts for 120 minutes with S.E.M. of 20 mice. (*$P<0.01$, **$P<0.001$ versus METH 1st). (b) Upper: Representative RT-PCR with 35 cycles for IL1β, IL-4, IL-6, IL-10, TNFα, TGFβ1, TGFβ2, TGFβ3, MCP1, RANTES, MCP3, CCR2, CXCL12 and CXCR4 mRNAs in the limbic forebrain of mice that have shown behavioral sensitization to methamphetamine (ME). The limbic forebrain sample was prepared 24 hours after the last injection of saline (SA) or ME. Lower: The intensity of the aforementioned bands was semi-quantified using Image J software. The value for mRNA was normalized by that for the internal standard glyceraldehyde-3-phosphate dehydrogenase (GAPDH) mRNA. The value for mice treated with methamphetamine is expressed as a percentage of the increase in mice treated with saline. Each column represents the mean ± SEM ($n=3$ animals per group; three independent experiments). N.D., not detectable. **$P<0.01$ versus saline-treated mice

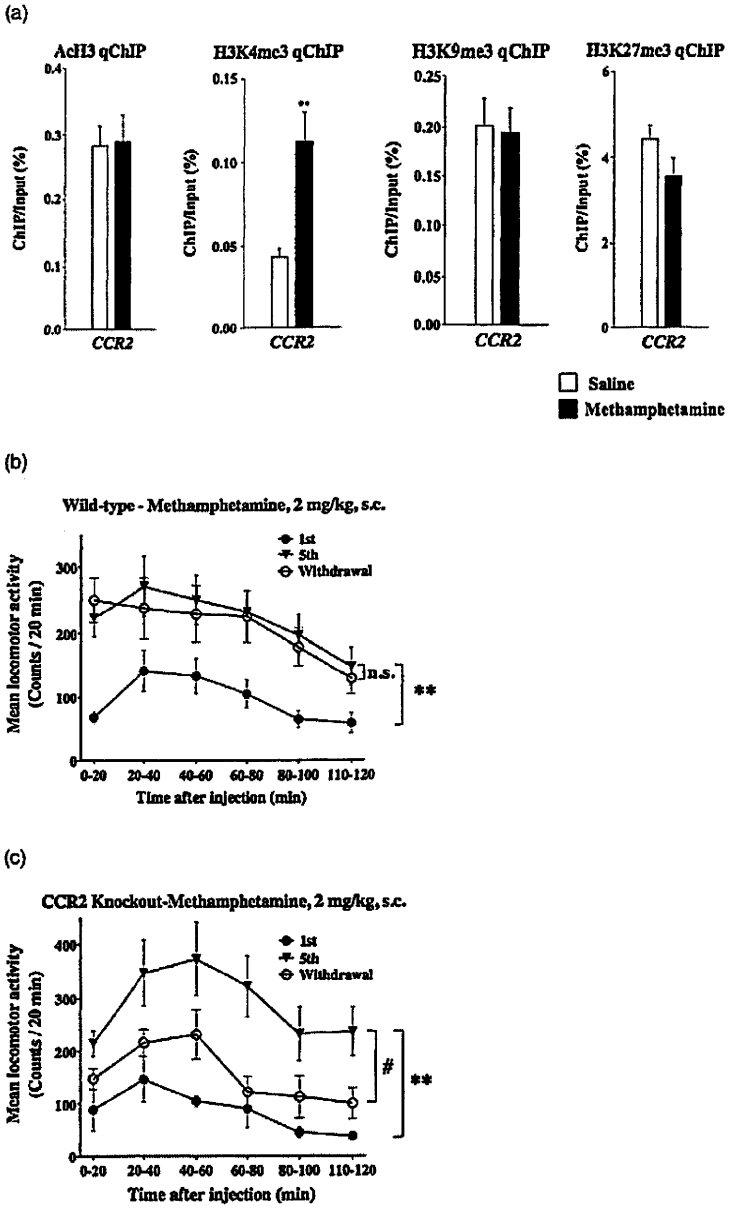

Figure 2 (a) qChIP analysis of acetylated histone H3 (AcH3), histone H3 trimethylated at lysine 4 (H3K4me3), lysine 9 (H3K9me3), and lysine 27 (H3K27me3) at CCR2 loci in the limbic forebrain of mice that had been intermittently treated with methamphetamine. Each column represents the mean ± SEM ($n = 4$ animals per group; three independent experiments). $^{**}P < 0.01$ versus saline-treated mice. (b) Change in locomotor activity (per 20 minutes time intervals) following intermittent administration of methamphetamine (2 mg/kg, s.c.) in wild-type mice (B-i) or CCR2 knockout mice (B-ii). Mice were treated intermittently with methamphetamine every 96 hours for five sessions. '1st' represents the 1st injection group, whereas 5th shows the 5th injection group. Mice described as 'withdrawal' were again administered methamphetamine after seven weeks of withdrawal. $^{**}P < 0.01$, 1st versus 5th, $\#P < 0.05$, 5th versus withdrawal (two-way ANOVA). n.s., not significant. Each point represents the mean ± SEM ($n = 4$–17 mice)

As shown in Fig. 1a, intermittent injection of methamphetamine produced a progressive increase in methamphetamine-induced locomotion, indicating the development of sensitization to methamphetamine (Fig. 1a, $F_{(4, 95)} = 4.940$, $P < 0.01$, first session versus fifth session).

As shown in Fig. 1b, a significant increase in mRNA of CCR2, but not of IL-1β, IL-4, IL-6, IL-10, TNFα, TGFβ1, TGFβ2, TGFβ3, MCP-1, RANTES, MCP-3, CXCL12 or CXCR4, was observed in the limbic forebrain, mainly including the nucleus accumbens, of the mice that had shown behavioral sensitization to methamphetamine (Fig. 1b, $P < 0.01$ versus the saline-treated mice). CCR2 is a seven-transmembrane-spanning Gαi protein-coupled receptor for a member of the C-C chemokine family, MCP-1, and is considered to regulate various brain disorders (Yong & Rivest 2009).

To gain further insight into these phenomena, we next studied histone modifications at the promoter regions of the CCR2 gene (Iida *et al.* 2008). A ChIP assay, where tissue is lightly fixed to crosslink DNA with histones and other DNA-binding proteins and then immunoprecipitated for a protein of interest, can be used to assess the extent to which a given gene is associated with these markers of activation or repression. In this study, we analyzed two active histone modifications [acetylation of

histone H3 and trimethylation of lysine 4 on histone H3 (H3K4)] and two repressive histone modifications [trimethylation of lysine 9 on histone H3 (H3K9) and trimethylation of lysine 27 on histone H3 (H3K27)] at the CCR2 gene promoter in the limbic forebrain of mice that had been intermittently treated with methamphetamine. As a result, intermittent treatment with methamphetamine caused a significant increase in the level of H3K4 trimethylation at the CCR2 promoter in the mouse limbic forebrain (Fig. 2a, $P < 0.01$ versus the saline-treated mice; Figs S1 and S2). Methamphetamine did not produce other histone modifications at the CCR2 gene promoter (Fig. 2a). To the best of our knowledge, the present data are the first to indicate that intermittent treatment with methamphetamine induces a dramatic increase in the expression of the CCR2 gene along with epigenetic modifications in the nucleus accumbens.

To address the functional relevance of the increased CCR2 expression after the intermittent administration of methamphetamine, we next investigated whether the reduction of CCR2 expression could affect behavioral sensitization to methamphetamine using CCR2 knockout mice (Fig. S3). As shown in Fig. 2b, the fifth injection of methamphetamine produced a dramatic and significant increase in methamphetamine-induced hyperlocomotion compared with the first injection in both C57BL/6J (wild-type) and CCR2 gene knockout mice to the same degree (wild-type: first versus fifth, $F_{(1, 160)} = 12.39$, $P < 0.01$, CCR2 knockout: first versus fifth, $F_{(1, 30)} = 20.00$, $P < 0.01$), indicating that lack of the CCR2 gene had little or no effect on the development of sensitization to methamphetamine-induced hyperlocomotion. Intriguingly, the sensitization to methamphetamine was maintained even after seven weeks of withdrawal following intermittent administration of methamphetamine in the wild-type mice (fifth versus withdrawal, $F_{(1, 110)} = 0.05$, no significant). However, the methamphetamine-induced sensitization was almost reversed after seven weeks of withdrawal in CCR2 knockout mice (fifth versus withdrawal, $F_{(1, 30)} = 8.50$, $P < 0.05$, Fig. 2b). These results indicate that CCR2 is implicated in the maintenance of behavioral sensitization to methamphetamine.

In conclusion, the present study suggests that the intermittent administration of methamphetamine increases the mRNA level of CCR2 in association with epigenetic modification at its promoter in the limbic forebrain including the nucleus accumbens, and this may correlate with the maintenance of sensitization to methamphetamine-induced hyperlocomotion.

References

Iida S, Watanabe-Fukunaga R, Nagata S, Fukunaga R (2008) Essential role of C/EBPalpha in G-CSF-induced transcriptional activation and chromatin modification of myeloid-specific genes. Genes Cells 13:313–327.

Renthal W, Nestler EJ (2008) Epigenetic mechanisms in drug addiction. Trends Mol Med 14:341–350.

Robinson TE, Kolb B (1999) Alterations in the morphology of dendrites and dendritic spines in the nucleus accumbens and prefrontal cortex following repeated treatment with amphetamine or cocaine. Eur J Neurosci 11:1598–1604.

Sokolov BP, Polesskaya OO, Uhl GR (2003) Mouse brain gene expression changes after acute and chronic amphetamine. J Neurochem 84:244–252.

Ujike H, Takaki M, Kodama M, Kuroda S (2002) Gene expression related to synaptogenesis, neuritogenesis, and MAP kinase in behavioral sensitization to psychostimulants. Ann N Y Acad Sci 965:55–67.

Vanderschuren LJ, Kalivas PW (2000) Alterations in dopaminergic and glutamatergic transmission in the induction and expression of behavioral sensitization: a critical review of preclinical studies. Psychopharmacology 151:99–120.

Yong VW, Rivest S (2009) Taking advantage of the systemic immune system to cure brain diseases. Neuron 64:55–60.

SUPPORTING INFORMATION

Additional Supporting Information may be found in the online version of this article:

Figure S1 qChIP analysis of acetylation of histone H3 (AcH3), H3K4me3, H3K9me3, and H3K27me3 in the limbic forebrain of mice that had been intermittently treated with methamphetamine (2 mg/kg, s.c., 5 times). Tubulin was used as a control for AcH3 and H3K4me3. High levels of AcH3 and H3K4me3 at the TATA box binding protein (Tbp) gene, which is transcriptionally activated within neurons, H3K9 and K27 trimethylation at silenced genes marker major satellite DNA, which probably comprises the functional centromere, and Gbx2 promoter (a homeobox-containing family of DNA-binding transcription factors) are seen in the limbic forebrain of methamphetamine-treated mice. Each column represents the mean ± S.E.M. ($n = 4$ animals per group; three independent experiments)

Figure S2 Representative PCR product with 40 cycles for CCR2 DNA in the limbic forebrain of mice that have shown behavioral sensitization to methamphetamine (ME). The limbic forebrain sample was prepared 24 hours after the last injection of saline (SA) or ME

Figure S3 Analysis of CCR2 mRNA expression by RT-PCR in the mouse whole brain from wild-type (WT) and CCR2 knockout (KO) mice

Table S1 Comprehensive list of all primer sequences used.

Appendix S1 Supplemental methods

Please note: Wiley-Blackwell are not responsible for the content or functionality of any supporting materials supplied by the authors. Any queries (other than missing material) should be directed to the corresponding author for the article.

PRECLINICAL STUDY doi:10.1111/j.1369-1600.2010.00249.x

Implication of dopaminergic projection from the ventral tegmental area to the anterior cingulate cortex in μ-opioid-induced place preference

Minoru Narita[1], Yuki Matsushima[1], Keiichi Niikura[1], Michiko Narita[1], Shigemi Takagi[1], Kae Nakahara[1], Kana Kurahashi[1], Minako Abe[1], Mai Saeki[1], Megumi Asato[1], Satoshi Imai[1], Kazutaka Ikeda[2], Naoko Kuzumaki[1] & Tsutomu Suzuki[1]

Department of Toxicology, Hoshi University School of Pharmacy and Pharmaceutical Sciences, Japan[1] and Division of Psychobiology, Tokyo Institute of Psychiatry, Japan[2]

ABSTRACT

Despite the importance of prefrontal cortical dopamine in modulating reward, little is known about the implication of the specific subregion of prefrontal cortex in opioid reward. We investigated the role of neurons projecting from the ventral tegmental area (VTA) to the anterior cingulate cortex (ACG) in opioid reward. Microinjection of the retrograde tracer fluorogold (FG) into the ACG revealed several retrogradely labelled cells in the VTA. The FG-positive reactions were noted in both tyrosine hydroxylase (TH)-positive and -negative VTA neurons. The released levels of dopamine and its major metabolites in the ACG were increased by either the electrical stimulation of VTA neurons or microinjection of a selective μ-opioid receptor (MOR) agonist, (D-Ala^2,*N*-MePhe^4,Gly-ol^5) enkephalin (DAMGO), into the VTA. MOR-like immunoreactivity was seen in both TH-positive and -negative VTA neurons projecting to the ACG. The conditioned place preference induced by intra-VTA injection of DAMGO was significantly attenuated by chemical lesion of dopaminergic terminals in the ACG. The depletion of dopamine in the ACG induced early extinction of μ-opioid-induced place preference. The levels of phosphorylated DARPP32 (Thr34) and phosphorylated CREB (Ser133) were increased in the ACG of rats that had maintained the morphine-induced place preference, whereas the increases of these levels induced by morphine were blocked by pre-treatment of a selective dopamine D1 receptor antagonist SCH23390. These findings suggest that VTA-ACG transmission may play a crucial role in the acquisition and maintenance of μ-opioid-induced place preference. The activation of DARPP32 and CREB through dopamine D1 receptors in the ACG could be implicated in the maintenance of μ-opioid-induced place preference.

Keywords Anterior cingulate cortex, dopamine, memory, opioid, μ-opioid receptor, reward.

Correspondence to: Minoru Narita, Department of Toxicology, Hoshi University School of Pharmacy and Pharmaceutical Sciences, 2-4-41 Ebara, Shinagawa-ku, Tokyo 142-8501, Japan. E-mail: narita@hoshi.ac.jp and suzuki@hoshi.ac.jp

INTRODUCTION

Studies on human addicts and behavioural studies in rodent models of addiction have indicated that key behavioural abnormalities associated with addiction are extremely long-lived. Drug of abuse is characterized by behavioural alternations in which compulsive drug seeking plays a central role. It is a chronic brain disorder as the risk of relapse remains high even after years of abstinence (Nestler 2001).

Brain dopamine systems have been the focus of histochemical, biochemical, and pharmacological research on the rewarding effects of and locomotor activity induced by opioids and psychostimulants. Dopaminergic neurons in the ventral tegmental area (VTA) innervate the nucleus accumbens (N.Acc), medial prefrontal cortex (mPFC), amygdala, hippocampus and ventral pallidum (Pierce & Kumaresan 2006). The ascending anatomical dopamine projection from the VTA to the N.Acc and mPFC is composed of mesocorticolimbic dopamine neurons (Koob 1992). Considerable evidence suggests that mesolimbic dopaminergic projections from the VTA to the N.Acc play an important role in the rewarding effects of drugs of abuse, including opioids (Kelley &

Berridge 2002). Altered function of the mPFC has been implicated in multiple processes and behavioural disorders, including schizophrenia (Weinberger 1995), drug abuse (Wise, Murray & Gerfen 1996), depression (Merriam *et al.* 1999) and attention deficit hyperactivity disorder (Puumala & Sirvio 1998) as well as normal cognitive processes, including working memory function (Williams & Goldman-Rakic 1995; Jentsch *et al.* 1997a,b) and decision making (Damasio 1995). The mPFC has received considerable attention with respect to its involvement in reward-related mechanisms (Tzschentke & Schmidt 2000). Noradrenaline (NA) release in the mPFC has been recently considered as crucial in mediating rewarding effects of opioids (Ventura, Alcaro & Puglisi-Allegra 2005). Despite the importance of prefrontal cortical dopamine, as well as NA, in modulating reward, cognition and behaviour, little is known about the involvement of dopamine that regulate the rewarding effects of opioids in the mPFC.

The anterior cingulate cortex (ACG), a major subregion of the prefrontal cortex, is involved in evaluative processes. The ACG might also serve to encode whether or not an action is worth performing in view of the expected benefit and the cost of performing the action (Rushworth *et al.* 2004). For instance, after excitotoxic ACG lesions, rats no longer selected the high cost–high reward option in a cost–benefit T-maze task if they had to choose between climbing a barrier to obtain a large reward in one arm or running for a low reward into the other arm with no barrier present (Walton *et al.* 2003). Recent studies have indicated that mesocortical dopamine fibres projecting to the ACG (Berger, Gaspar & Verney 1991) may be responsible for effort-based decision-making (Schweimer, Saft & Hauber 2005). In addition, the ACG contributes to the generation of emotional states and to the executive control of behavioural selection (Peoples 2002).

In the present study, we therefore investigated the role of dopaminergic neurons projecting from the VTA possibly to the ACG in μ-opioid reward.

MATERIALS AND METHODS

The present study was conducted in accordance with the Guiding Principles for the Care and Use of Laboratory Animals (Hoshi University) as adopted by the Committee on Animal Research of Hoshi University, which is accredited by the Ministry of Education, Culture, Sports, Science, and Technology of Japan. Every effort was made to minimize the number and suffering of animals used in the following experiments.

Animals

In the present study, we used male Sprague Dawley rats (200–250 g) (Tokyo Laboratory Animals Science, Tokyo, Japan). The animals were housed in a room maintained at 23 ± 1°C with a 12-hour light/dark cycle (lights on 8 AM to 8 PM). Food and water were available *ad libitum*.

Drugs

The drugs used in the present study were morphine hydrochloride (Daiichi-Sankyo, Tokyo, Japan), 6-hydroxydopamine hydrochloride (6-OHDA), desipramine hydrochloride, (D-Ala^2, *N*-MePhe^4, Gly-ol^5) enkephalin (DAMGO) (Sigma-Aldrich, St. Louis, MO), R(+)-7-chloro-8-hydroxy-3-methyl-1-phenyl-2,3,4,5-tetrahydro-1H-3-benzazepine hydrochloride (SCH23390; Sigma Chemical Co., MO, USA), fluorogold (FG; fluorochrome, Englewood, CO, USA), and cholera toxin B Alexa Fluor 555 conjugate (CTb; Invitrogen, Grand Island, NY, USA).

Experiments I

In retrograde tracing study, the rats were deeply anesthetized with sodium pentobarbital (50 mg/kg, i.p.) and placed in a stereotaxic apparatus. The skull was exposed, and a hole was drilled through the skull over the ACG (from bregma: anterior +1.7 mm; lateral +0.4 mm; and ventral −2.8 mm) or N.Acc (from bregma; anterior +1.5 mm; lateral +2.7 mm; and ventral −7.3 mm; angle 10°) according to the atlas of Paxinos and Watson (Paxinos & Watson 1998). Except pressure-injected (200 nl) into the ACG in the FG (fluorochrome, 4% solution in saline) injection, micropipettes of about 20–23 μm in diameter were filled with FG solution, and the tracer was injected into the N.Acc for 25 minutes by iontophoresis with a positive-pulsed current (5 μA, seven seconds on/off intervals). The micropipette was left in place for five minutes following the completion of injection to avoid leakage of the tracer along the pipette track, and then the pipette was withdrawn from the brain. In the CTb (Invitrogen) injection, the injection cannula was filled with CTb (1 mg/ml) solution, and CTb was pressure-injected (1 μl) into the ACG. The CTb, as well as FG, was used as retrograde tracer (Kishi *et al.* 2006; Almarestani *et al.* 2007; Steen *et al.* 2007). After the injection, the injection cannula was left in place for five minutes. Five days after the injections, the animals were perfused as described later. The distributions of FG or CTb retrogradely labelled neurons and FG or CTb injection sites were detected using a microscope (Olympus BX-60; Olympus, Tokyo, Japan). In perfusion and tissue processing, the rats were deeply anesthetized with 3% isoflurane and perfusion-fixed with 4% paraformaldehyde, pH 7.4. The brains were then quickly removed after perfusion, and thick coronal sections of the ACG, N.Acc or VTA were initially dissected using brain blocker (Neuroscience, Tokyo, Japan). The brain coronal sections were post-fixed in 4% paraformaldehyde for three hours. After the brains

were permeated with 20% sucrose for one day and 30% sucrose for two days, they were frozen in embedding compound (Sakura Finetechnical, Tokyo, Japan) on isopentane using liquid nitrogen and stored at −30°C until use. Frozen 8 μm-thick coronal sections were cut with a cryostat (CM1510; Leica, Heidelberg, Germany) and thaw-mounted on poly-L-lysine-coated glass slides. In immunohistochemical approach, the brain sections were blocked in serum in 0.01 mol/l phosphate buffer saline (PBS) for one hour at 23 ± 1°C. Each primary antibody was diluted in 0.01 mol/l PBS containing 10% normal goat serum (NGS) [1:25, 1:40 or 1:60 tyrosine hydroxylase (TH; mouse monoclonal, MAB358, Chemicon, Temecula, CA, USA)] and incubated for two days at 4°C. The samples were then rinsed and incubated with the appropriate secondary antibody conjugated with Alexa 488 and Alexa 546 for two hours at 23 ± 1°C. The slides were then coverslipped with PermaFluor Aqueous mounting medium (Immunon, Pittsburgh, PA, USA). Fluorescence of immunolabelling was detected using a light microscope (Olympus BX-60) and U-MWIG and U-MNIBA filter cubes (Olympus) for an Alexa 488 or Alexa 546. Digitized images of the ACG, N.Acc or VTA sections were captured at a resolution of 1316 × 1035 pixels with a camera (Polaroid PDMCII/OL; Olympus). The upper and lower threshold density ranges were adjusted to encompass and match the immunoreactivity (IR) to provide an image in which IR material appeared as white pixels and non-IR material appeared as black pixels.

Experiments II

In surgery and microinjection, after three days of habituation to the main animal colony, all of the rats were anesthetized with sodium pentobarbital (50 mg/kg, i.p.). The anesthetized animals were placed in a stereotaxic apparatus. The skull was exposed, and a small hole was made using a dental drill. A guide cannula (AG-9, AG-8 or AG-4; Eicom, Kyoto, Japan) or an electrode (NS303/12; Bioresearch Center, Nagoya, Japan) was implanted into the VTA (from bregma: anterior, −5.3 mm; lateral, −0.9 mm; ventral, −7.7 mm or anterior, −6.8 mm; lateral, ±0.9 mm; ventral, −7.8 mm; angle 10°), ACG [from bregma: anterior, +1.7 mm; lateral, −0.4 mm; ventral, −1.1 mm (*in vivo* microdialysis) or −2.3 mm (microinjection)] or N.Acc (from bregma; anterior, +4.0 mm; lateral, −0.8 mm; ventral, −6.8 mm; angle 16°) according to the atlas of Paxinos & Watson (1998). The guide cannula or the electrode was fixed to the skull with cranioplastic cement. In the microinjection method, we used an injection cannula (AMI-9.5; Eicom) that extended beyond the guide cannula by 0.5 mm. A stainless steel injection cannula was inserted into the guide cannula for each animal. The injection cannula was connected through polyethylene tubing to a 10 μl Hamilton syringe that was preloaded with DAMGO (1 nmol/0.3 μl) or saline. DAMGO or saline was delivered by a motorized syringe pump in a volume of 0.3 μl over 60 seconds. In *in vivo* microdialysis study, three to five days after the surgery, microdialysis probes (AI-4-2 or AI-8-2; 2 mm membrane length; Eicom) were slowly inserted into the ACG or N.Acc through guide cannulas under anaesthesia with diethyl ether, and the rats were settled in the experimental cages (30 cm wide × 30 cm deep × 30 cm high). The probes were perfused continuously at a flow rate of 2 μl/minute with artificial cerebrospinal fluid (aCSF) containing 0.9 mM $MgCl_2$, 147.0 mM NaCl, 4.0 mM KCl and 1.2 mM $CaCl_2$. The outflow fractions were taken every 20 minutes. After three baseline fractions were collected in the rat ACG or N.Acc, DAMGO or saline was administered into the rat VTA using a 10 μl Hamilton syringe and a motorized syringe pump. For these experiments, dialysis samples were collected for 180 minutes after DAMGO or saline treatment. Dialysis fractions were then analyzed using HPLC (Eicom) with an electrochemical detection (ECD) (Eicom) system. Dopamine was separated by a column with a mobile phase containing sodium acetate (4.05 g/l), citric acid monohydrate (7.35 g/l), sodium 1-octane sulfonate (150 mg/l), EDTA (2Na; 10 mg/l) and 17% methanol. The mobile phase was delivered at a flow rate of 210 μl/minute. Dopamine was identified according to the retention time of a dopamine standard, and the peak area of basal dopamine was divided by the peak area of a dopamine standard to obtain the amount of basal dopamine. In electrical stimulation, three to five days after surgery, microdialysis probes were inserted and an *in vivo* microdialysis study was performed as described earlier. Electrical stimulation (stimulation intensity of 100 or 150 μA, stimulation frequency of 100 Hz, 0.5-second trains of 0.5-m second pulses, interval of two seconds) was applied to the VTA for 40 minutes after three baseline fractions were collected in the rat ACG. This stimulation was delivered by constant-current stimulators via a bipolar cable (Bioresearch Center) connected to the electrode.

Experiments III

Immunohistochemical study was conducted as described earlier. Each primary antibody was diluted in 0.01 mol/l PBS containing 10% NGS [1:25, 1:40 or 1:60 tyrosine hydroxylase (mouse monoclonal, MAB358)] or 20% NGS in 0.1% Triton X-100 [1 : 3500 MOR (rabbit polyclonal, RA10104, Neuromics, Bloomington, MN, USA)]. The microinjection of retrograde tracer was conducted as described earlier.

Experiments IV

Place conditioning was conducted as described previously (Suzuki, Masukawa & Misawa 1990). The biased

design was used for place conditioning. The apparatus was a shuttle box (30 cm wide × 60 cm long × 30 cm high) that was made of acrylic resin board and divided into two equal-sized compartments. One compartment was white with a textured floor, and the other was black with a smooth floor to create equally preferable compartments. The place conditioning schedule was composed of three phases (pre-conditioning test, conditioning, and post-conditioning test). The pre-conditioning test was performed as follows: the partition separating the two compartments was raised to 12 cm above the floor, a neutral platform was inserted along the seam separating the compartments and the animals that had not been treated with either drugs or saline were then placed on the platform. The time spent in each compartment during a 900-seconds session was then recorded automatically with an infrared beam sensor (KN-80; Natsume Seisakusyo, Tokyo, Japan). Conditioning sessions (three days for DAMGO (0.3, 1, 3, 9 nmol/0.3 μl) or morphine (8 or 23 mg/kg, i.p.), three days for saline) were conducted once daily for six days. Immediately after DAMGO injection or treatment with morphine, these animals were placed in the compartment opposite that in which they had spent the most time in the pre-conditioning test for one hour. On alternating days, these animals received saline and were placed in the other compartment for one hour. On the day after the final conditioning session, a post-conditioning test that was identical to the pre-conditioning test was performed. To destroy central dopaminergic neurons, 6-OHDA (8 μg/0.3 μl) was injected into the ACG of the rats four days before the start of conditioning with DAMGO or morphine. Additionally, desipramine (20 mg/kg, s.c.) was given to rats 30 minutes before the injection of 6-OHDA into the ACG to block the uptake of 6-OHDA into noradrenergic terminals (Alhaider 1991). To investigate the extinction of the morphine- or DAMGO-induced place preference, a post-conditioning test was performed with no conditioning and was conducted at 1 day, 9 days, 13 days or 20 days after the final conditioning test. Immunohistochemical study was conducted as described earlier. Primary antibody was diluted in 0.01 mol/l PBS containing 10% NGS [1:1000 TH (rabbit polyclonal, AB152, Chemicon)]. In high-pressure liquid chromatography (HPLC) study, the rats were killed four days after the microinjection of saline or 6-OHDA (8 μg/0.3 μl) in combination with s.c. injection of vehicle or desipramine. The brain was removed quickly, and the ACG was dissected on an ice-cold glass plate. The tissues were homogenized in 1000 μl of 0.2 M perchloric acid containing 100 mM EDTA(2Na) and 140 ng isoproterenol as an internal standard. The homogenates were then centrifuged at 20 000 ×g for 32 minutes at 4°C, and the supernatants were maintained at pH 3.0 using 1 M sodium acetate. The samples were analyzed by HPLC-ECD. The HPLC system was composed of a delivery system (EP-10; Eicom), an analytical column (Eicompac, SC-5ODS; Eicom) and a guard column (Eicom). Dopamine and its metabolites were separated by a column with a mobile phase containing sodium acetate (3.22 g/l), citric acid monohydrate (9.17 g/l), sodium 1-octane sulfonate (180 mg/l), EDTA(2Na) (10 mg/l) and 17% methanol. The mobile phase was delivered at a flow rate of 0.5 ml/minute. Dopamine and its metabolites were identified according to the retention times of these standards, and the peak heights of dopamine and its metabolites revised internal standard was divided by the peak heights of those standard revised internal standard to obtain those amount.

Experiments V

Place conditioning was performed as described earlier. In treatment with SCH23390, the rats were administered saline or SCH23390 (0.1 mg/kg, i.p.) 15 minutes before the treatment with morphine. In Western blotting, 24 hours or 10 days after the final conditioning in the conditioned place preference (CPP) procedure described earlier, the rats were sacrificed by decapitation. The ACG was quickly removed after decapitation and homogenized in ice-cold buffer. The homogenate was centrifuged at 20 000 ×g for 10 minutes and the supernatant was retained as the lysate fraction for Western blotting. An aliquot of tissue sample was diluted with an equal volume of 2× electrophoresis sample buffer (Protein Gel Loading Dye-2X, Amresco, Solon, OH, USA) containing 2% sodium dodecyl sulfate (SDS) and 10% glycerol with 0.2 M dithiothreitol. Proteins (7 μl/lane) were separated by size on 4–20% SDS-polyacrylamide gradient gel by using the buffer system of Laemmli (1970) and transferred to nitrocellulose membranes in Tris-glycine buffer containing 25 mM Tris and 192 mM glycine. For immunoblot detection, the membranes were blocked in Tris-buffered saline (TBS) containing 1% non-fat dried milk (Bio-Rad Laboratories, Hercules, CA, USA) containing 0.1% Tween 20 (Research Biochemicals, Natick, MA, USA) for one hour at room temperature with agitation. The membrane was incubated with primary antibody diluted in 1:1000 phosphorylated dopamine and cyclic AMP-regulated phosphoprotein with molecular weight 32 kDa (p-DARPP32; rabbit, #2304, Cell Signaling Technology, Danvers, CA, USA) and 1:1000 phosphorylated cAMP response element binding protein (p-CREB; rabbit, #9191, Cell Signaling Technology), 1:200 000 glyceraldehyde-3-phosphate dehydrogenase (GAPDH; mouse monoclonal, MAB374, Chemicon International, Temecula, CA, USA) containing 1% non-fat dried milk containing 0.1% Tween 20 overnight at 4°C. The membrane was washed in TBS containing 0.05% Tween 20

(TTBS), and then incubated for two hours at room temperature with horseradish peroxidase-conjugated goat anti-rabbit IgG (Southern Biotechnology Associates, Birmingham, AL, USA) diluted 1:10 000 in TBS containing 1% non-fat dried milk with 0.1% Tween 20. After this incubation, the membranes were washed in TTBS. The antigen-antibody peroxidase complex was finally detected by enhanced chemiluminescence (Pierce, Rockford, IL, USA) according to the manufacturer's instructions and visualized by exposure to Amersham Hyperfilm (Amersham Life Sciences, Arlington Heights, IL, USA).

Histology

The locations of the infusion cannula and drug diffusion were assessed at the completion of the experiments. The rats were deeply anesthetized with sodium pentobarbital at the end of the experiment and given microinjections of ink for the anatomical localization of cannula sites (0.3 μl). The brain was then removed by decapitation and cut into coronal sections. Cannula locations were mapped onto a stereotaxic atlas (Paxinos & Watson 1998) and confirmed to be in the VTA, ACG or N.Acc.

Statistical data analysis

Dates are expressed as the mean with SEM. One- and two-way analyses of variance (ANOVAs) with independent and repeated measures as well as planned comparisons or Student's *t*-tests, were used as appropriate for the experimental design. Multiple comparisons were performed using Dunnet or Bonferroni *post hoc* test where appropriate. The potency ratio for the saline-treated rats and the 6-OHDA-treated rats were calculated by the parallel line assay (Tallarida, Porreca & Cowan 1989).

RESULTS

Experiments I

Dopamine neurons projecting from the VTA to the ACG

To determine whether the VTA is linked to the ACG, we investigated whether there were any neuronal projections from the VTA to the ACG using FG as a retrograde tracer. Schematic illustrations of the injection site in the ACG (CG1, CG2) or N.Acc are shown with the symbols (Fig. 1a, b). Pressure application of FG into the region of the unilateral ACG produced a well-restricted injection site (Fig. 1c). FG-labelled cell bodies (Fig. 1d) or TH-labelled cells (Fig. 1e) were apparently detected in the VTA after the microinjection of FG into the ACG. A population of retrogradely labelled neurons in the VTA also showed TH-IR (Fig. 1f).

Distribution of cell bodies of neurons projecting from the VTA to the ACG or N.Acc

To investigate whether neurons that projected from the VTA to the ACG or N.Acc were independent, the retrograde tracers CTb and FG were microinjected into the unilateral ACG and N.Acc, respectively (Fig. 1g, h). FG- or CTb-containing cells were detected in the VTA after the microinjection of FG or CTb. FG-labelled neurons and CTb-labelled neurons did not overlap in the VTA (Fig. 1i).

Experiments II

Dialysate dopamine level in the ACG by electrical stimulation in the VTA

To further verify the dopaminergic neurons projecting from the VTA to the ACG, we examined the effect of the electrical stimulation of VTA cells on dopamine release in the ACG. In an *in vivo* microdialysis study, the basal levels of dopamine and the major dopamine metabolites, 3,4-dihydroxyphenylacetic acid (DOPAC) and homovanillic acid (HVA), in the ACG were lower than that of dopamine in the N.Acc ($n = 5$) (*$P < 0.05$, **$P < 0.01$ versus dopamine, DOPAC or HVA in the N.Acc) (Table 1). The dopamine levels in the ACG were increased by the electrical stimulation of VTA cells ($n = 5$) (Fig. 2a). The electrical stimulation of VTA cells also increased the levels of DOPAC and HVA ($n = 5$) (Fig. 2b, c). Statistical analysis was performed with one-way ANOVA followed by Dunnet test (dopamine, $F_{(7,28)} = 3.710$, $P < 0.01$; DOPAC, $F_{(7,28)} = 7.426$, $P < 0.001$; HVA, $F_{(7,28)} = 12.04$, $P < 0.001$) (*$P < 0.05$, **$P < 0.01$, ***$P < 0.001$ versus 0 minute).

Dialysate dopamine level in the ACG under the microinjection of a μ-opioid receptor agonist into the VTA

We next investigated the change in the dialysate dopamine level in the ACG under the intra-VTA administration of a μ-opioid receptor agonist. Schematic illustrations of dialysis probe placements in the ACG or N.Acc are shown in Fig. 3a, b. The dopamine level was markedly increased by the injection of DAMGO compared with saline treatment in the ACG ($n = 5$) (Fig. 3c). The injection of DAMGO into the VTA also produced a significant increase in DOPAC and HVA in the ACG ($n = 5$) (Fig. 3d, e). Statistical analysis was performed with two-way ANOVA followed by Bonferroni test [dopamine: interaction between treatment and time: $F_{(11,88)} = 1.972$, $P < 0.05$; effect of treatment, $F_{(1,88)} = 5.841$, $P < 0.05$; effect of time, $F_{(11,88)} = 3.250$ $P < 0.001$; DOPAC: interaction between treatment and time: $F_{(11,88)} = 7.278$, $P < 0.001$; effect of treatment, $F_{(1,88)} = 22.77$, $P < 0.01$; effect of time, $F_{(11,88)} = 12.60$, $P < 0.001$; HVA: interaction between treatment and time: $F_{(11,88)} = 3.823$, $P < 0.001$; effect

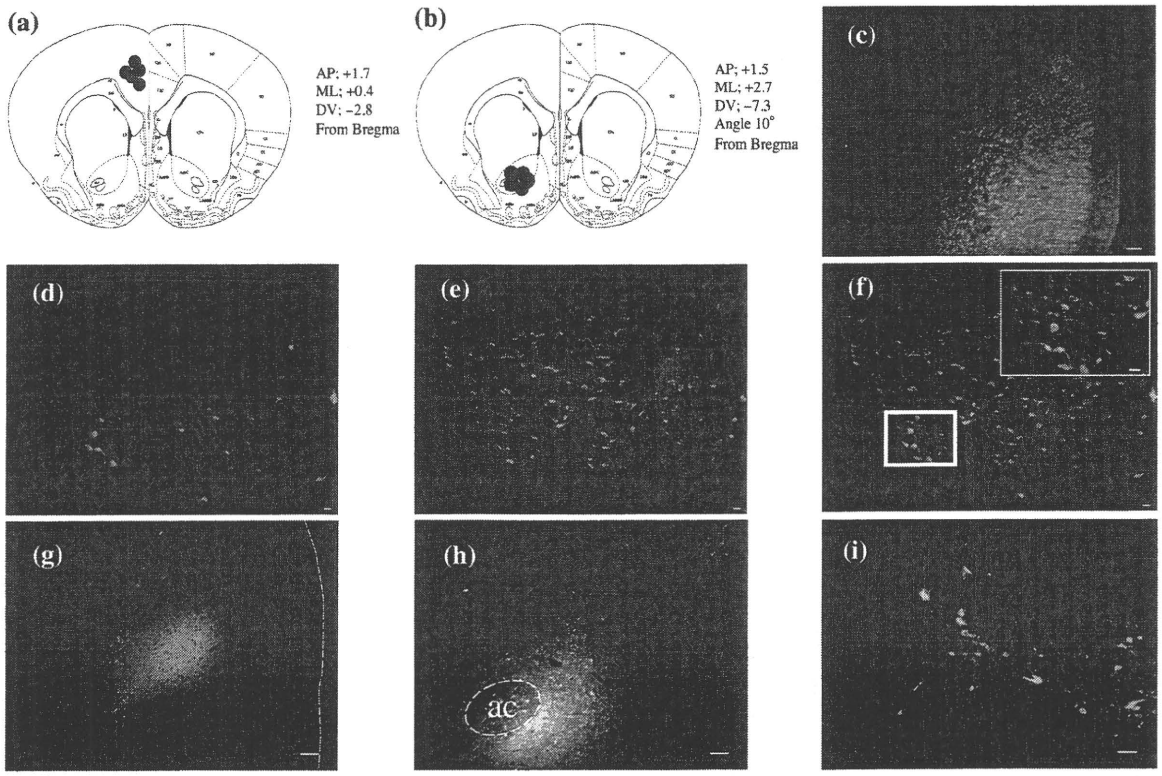

Figure 1 Projection of dopamine neurons from the ventral tegmental area (VTA) to the anterior cingulate cortex (ACG) and the distribution of cell bodies in the VTA projecting to the ACG or N.Acc of rats. (a–b) Schematic illustrations of the injection site (symbols) in the ACG (a) or N.Acc (b). (c) The image shows the extent of fluorogold (FG) diffusion at the injection site. (d) Cells in the VTA after the microinjection of FG into the ACG. (e) Tyrosine hydroxylase (TH)-IR was noted in the VTA. (f) Double-labelling experiments showed that FG-positive cells overlapped TH-positive cells in the VTA. (g) The extent of cholera toxin B diffusion at the injection site in the ACG. (h) The extent of FG diffusion at the injection site in the N.Acc; ac = anterior commissure. (i) Cells in the VTA after the microinjection of FG into the ACG and cholera toxin B into the N. Acc. Double-labelling experiments showed that FG-positive and cholera toxin B-positive cells did not overlap in the VTA. Scale bars, 50 μm

Table 1 Basal dialysate levels of dopamine and its metabolites in the nucleus accumbens or anterior cingulated cortex and the decrease in the contents of dopamine and its metabolites in the anterior cingulated cortex in desipramine-6-OHDA-treated rats.

	Dopamine	*DOPAC*	*HVA*
Brain area (nM)[a]			
Nucleus accumbens	0.8 ± 0.2	374.9 ± 86.2	109.7 ± 17.8
Cingulate cortex	0.2 ± 0.1*	19.2 ± 4.5**	24.3 ± 3.3**
Group (ng/g wet tissue)[b]			
Vehicle-saline	100.2 ± 0.901	34.7 ± 2.547	71.3 ± 1.678
Desipramine-6-OHDA	75.6 ± 0.396***	21.6 ± 0.514***	44.2 ± 0.450***

[a]Each value represents the mean ± SEM. The data were calculated as concentrations in the dialysates for five rats. *$P < 0.05$, **$P < 0.01$ versus dopamine, DOPAC or HVA in the N.Acc.
[b]Each value represents the mean ± SEM. The rats were killed four days after the microinjection of saline or 6-OHDA into the ACG. The data were calculated as dopamine and its metabolited contents in the ACG for four rats. The statistical significance of differences between groups was assessed with Student's *t*-test. ***$P < 0.001$ versus vehicle-saline.

of treatment, $F_{(1,88)} = 5.355$, $P < 0.05$; effect of time, $F_{(11,88)} = 2.567$, $P < 0.01$) (*$P < 0.05$, ***$P < 0.001$, saline versus DAMGO]. The dopamine and its metabolite levels were markedly increased by the injection of DAMGO compared with saline treatment in the N.Acc ($n = 5$) (Fig. 3f, g, h). Statistical analysis were performed with two-way ANOVA followed by Bonferroni test [dopamine: interaction between treatment and time: $F_{(11,88)} = 5.404$, $P < 0.001$; effect of treatment, $F_{(1,88)} = 8.963$, $P < 0.05$; effect of time, $F_{(11,88)} = 3.450$, $P < 0.001$; DOPAC: interaction between treatment and time: $F_{(11,88)} = 33.18$, $P < 0.001$; effect of treatment,

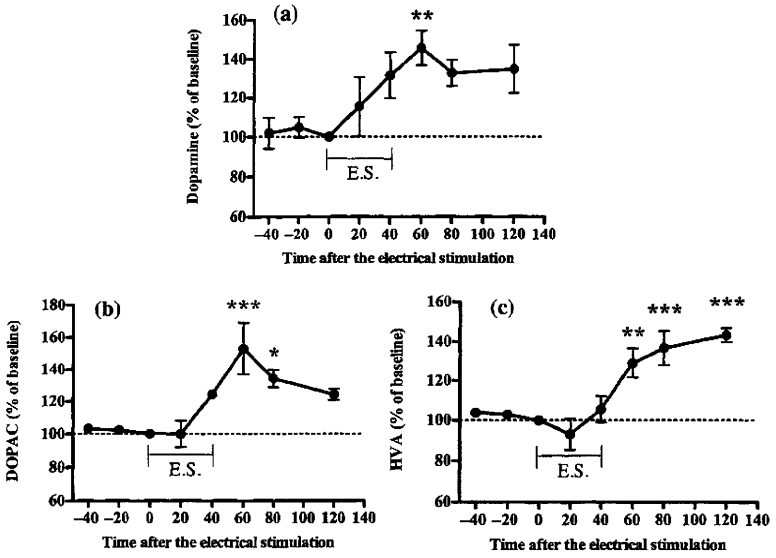

Figure 2 Change in the dialysate levels of dopamine and its metabolites induced by electrical stimulation (ES) in the rat VTA. (a–c) Effect of ES on the dialysate dopamine (a), DOPAC (b) and HVA (c) levels in the ACG in rats. The rats were subjected to electrical stimulation at time 0 for 40 minutes. The data are expressed as percentages of the corresponding baseline levels with SEM of the five rats. Dunnet test: $^{*}P < 0.05$, $^{**}P < 0.01$, $^{***}P < 0.001$ versus 0 minute

$F_{(1,88)} = 50.84$, $P < 0.001$; effect of time, $F_{(11,88)} = 29.78$, $P < 0.001$; HVA: interaction between treatment and time: $F_{(11,88)} = 17.02$, $P < 0.001$; effect of treatment, $F_{(1,88)} = 24.11$, $P < 0.01$; effect of time, $F_{(11,88)} = 12.12$, $P < 0.001$) ($^{*}P < 0.05$, $^{**}P < 0.01$, $^{***}P < 0.001$, saline versus DAMGO].

Experiments III

Distribution of μ-opioid receptors in the VTA

We next investigated the distribution of MOR-IR in the VTA after the microinjection of FG into the ACG. FG-, MOR- or TH-labelled cells were detected in the VTA (Fig. 4a, b, c). A triple labelling experiment showed that MOR-IR in the VTA was detected on both TH- and non-TH-labelled neurons with a FG-positive reaction (Fig. 4e, f). Some MOR-labelled neurons with no FG reaction did not show TH-IR (Fig. 4g). Percentages of MOR, TH and FG labels, individually and in combination, in the VTA are shown in Fig. 4h.

Experiments IV

Role of VTA-ACG dopaminergic neurons in the acquisition and maintenance of the place preference induced by the μ-opioid receptor agonist

To investigate the involvement of VTA-ACG dopaminergic neurons in the induction of opioid reward, the rats were microinjected with 6-hydroxydopamine (6-OHDA) into the ACG after the s.c. injection of desipramine to specifically deplete dopamine. Pre-microinjection of 6-OHDA in combination with the s.c. administration of desipramine markedly decreased the basal levels of dopamine and its metabolites in the rat ACG ($^{***}P < 0.001$ versus vehicle-saline) ($n = 4$) (Table 1), whereas it failed to change the basal levels of dopamine and its metabolites in the N.Acc (Saline; $n = 6$, 6-OHDA; $n = 5$) [Dopamine: 88.8 ± 16.0 (% of control); DOPAC: 107.8 ± 15.7 (% of control); HVA: 98.0 ± 18.1 (% of control)]. The microinjection of 6-OHDA into the ACG after the treatment with desipramine did not affect NA and serotonin (5-HT) contents in the ACG [(NA: saline; 281.6 ± 11.6, 6-OHDA; 206.8 ± 14.7, NS, 5-HT: saline; 51.8 ± 1.4. 6-OHDA; 64.9 ± 5.1, NS (ng/g weight tissue)]. The injury of dopaminergic neurons, by 6-OHDA injection in the ACG, reduced TH-IR in the VTA ($^{*}P < 0.05$ versus saline) (Fig. 5a–c). In the CPP method, the microinjection of DAMGO into the VTA produced a dose-dependent place preference. The DAMGO-induced place preference was attenuated by the pre-microinjection of 6-OHDA into the ACG. The concentration-response line for the 6-OHDA-pre-treated group was shifted to the right compared with that for the saline-pre-treated group. The potency ratio of the place preference induced by DAMGO in saline-pre-treated group versus 6-OHDA-pre-treated group was 3.32 (saline: 0.3 nmol, $n = 7$; 1 nmol, $n = 6$; 3 nmol, $n = 8$, 6-OHDA: 1 nmol, $n = 8$; 3 nmol, $n = 6$; 9 nmol, $n = 6$) (Fig. 5d). The saline or the 6-OHDA pre-treated control rats failed to show the place preference (saline–saline: −36.9 ± 48.1, $n = 6$; 6-OHDA-saline: 22.7 ± 57.7, $n = 6$). Under these conditions, the 6-OHDA-pre-treated rats that produced the right shift of concentration–response line of the DAMGO-induced place preference showed extinction of the place preference at nine days after the final conditioning, whereas the place preference induced by the microinjection of DAMGO into the VTA in saline-pre-treated rats was maintained at nine days (Fig. 5e). Statistical analysis was performed with two-way ANOVA [saline; interaction between dose and day: $F_{(1,12)} = 0.6581$, NS; effect of dose, $F_{(1,12)} = 2.856$, NS;

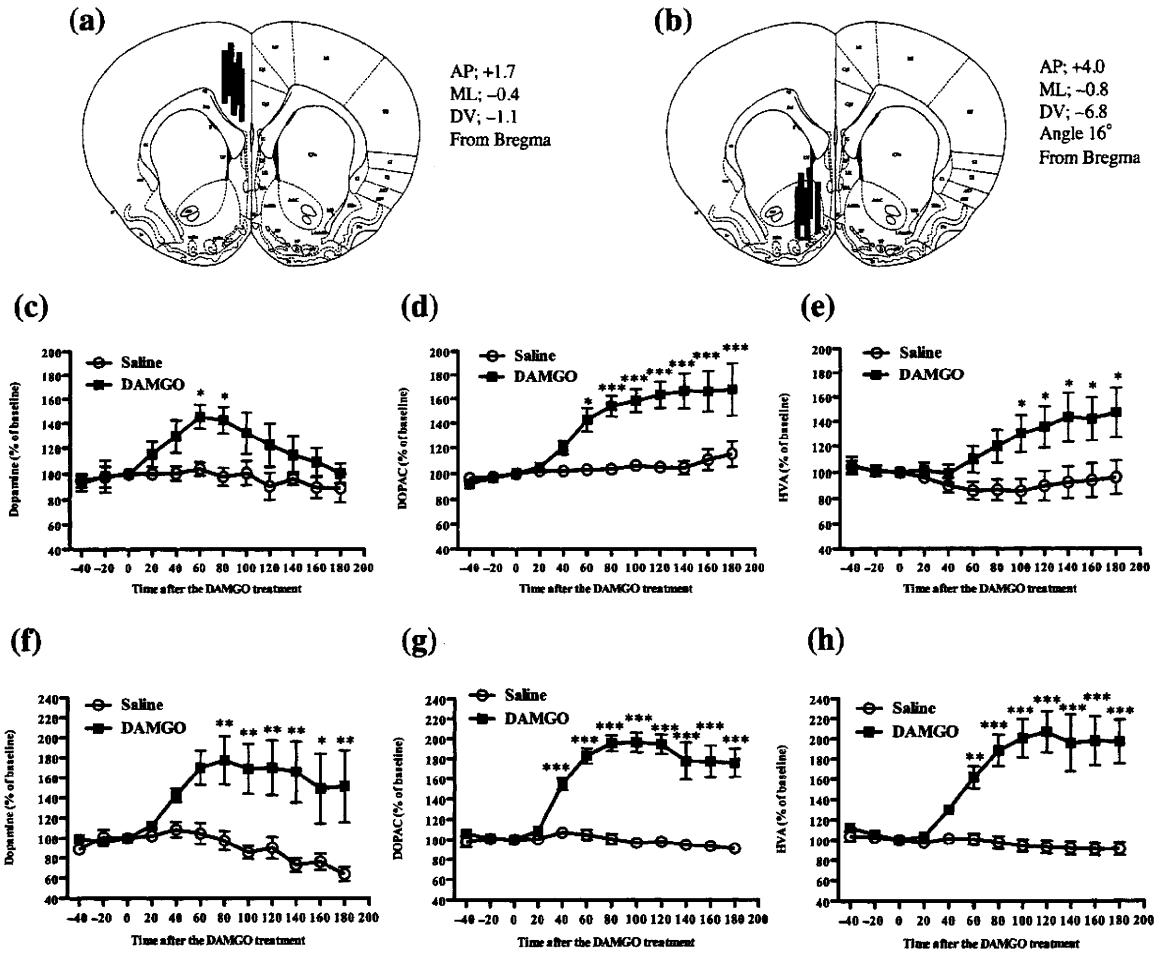

Figure 3 Change in the dialysate levels of dopamine and its metabolites induced by DAMGO administration into the VTA. (a–b) Schematic illustrations of the dialysis probe locations in the ACG (a) or N.Acc (b). (c–e) Effects of DAMGO administration into the VTA on the dialysate levels of dopamine (c) and its metabolites (d, e) in the ACG. After baseline fractions were collected, saline or DAMGO (1 nmol) was administered into the VTA at time 0 to evoke the release of dopamine. Data are expressed as percentages of the corresponding baseline levels with SEM for five rats. (f–h) Effects of DAMGO administration into the VTA on the dialysate levels of dopamine (f) and its metabolites (g, h) in the N.Acc. Data are expressed as percentages of the corresponding baseline levels with SEM for the five rats. Bonferroni test: $^{*}P < 0.05$, $^{**}P < 0.01$, $^{***}P < 0.001$, saline versus DAMGO

effect of day, $F_{(1,12)} = 0.02324$, NS, 6-OHDA; interaction between dose and day: $F_{(1,10)} = 0.9401$, NS; effect of dose, $F_{(1,10)} = 1.005$, NS; effect of day, $F_{(1,10)} = 14.57$, $P < 0.01$]. The saline- or 6-OHDA- pre-treated control rats failed to show the place preference at nine days after the final conditioning (saline–saline: -2.8 ± 45.1, $n = 6$; 6-OHDA-saline: 40.8 ± 36.6, $n = 6$). Furthermore, the 6-OHDA- pre-treated rats that received 23 mg/kg of morphine (i.p.), which exhibited the almost same score to that observed in the rats receiving 8 mg/kg of morphine (i.p.) showed early extinction after the post-test, whereas the saline-pre-treated rats that received 8 mg/kg of morphine failed to exhibit extinction of its place preference ($n = 6$). Statistical analysis was performed with two-way ANOVA [interaction between treatment and time: $F_{(3,30)} = 2.150$, NS; effect of treatment, $F_{(1,30)} = 5.284$, $P < 0.05$; effect of time, $F_{(3,30)} = 4.220$, $P < 0.05$] (Fig. 5f).

Experiments V

Activation of DARPP32 and CREB in the ACG of rats that maintained the μ-opioid-induced place preference

We next investigated whether the acquisition or maintenance of morphine-induced place preference could be associated with the phosphorylation of DARPP32 and CREB, which are the downstream of dopamine D1 receptor signalling in the ACG. The acquisition of morphine-induced place preference at 24 hours after the final conditioning was attenuated by pre-treatment of a

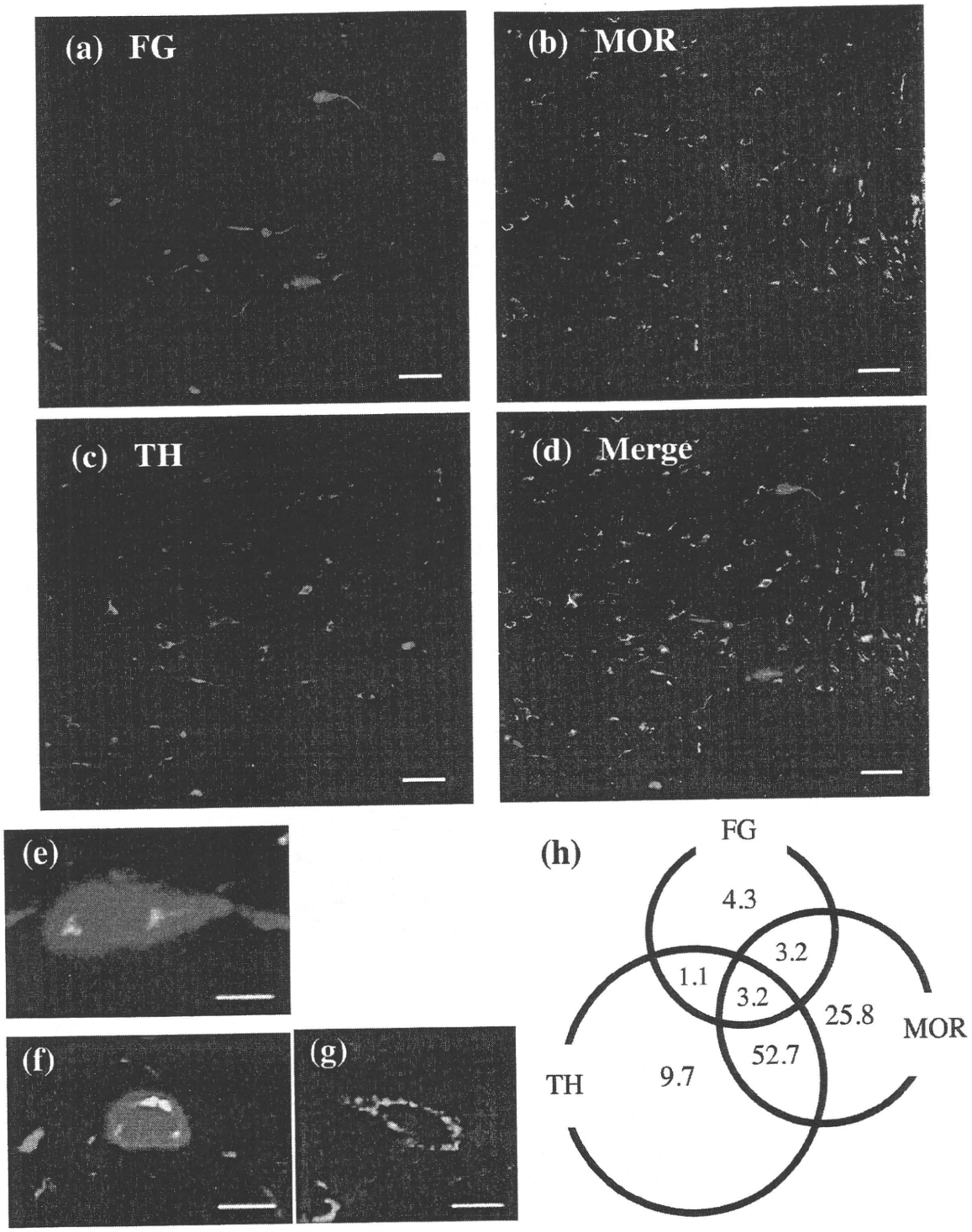

Figure 4 Characterization of μ-opioid receptors (MORs) in the VTA. (a) Cells in the VTA after the microinjection of FG into the ACG. (b) MOR-IR was noted in the VTA. (c) TH-IR was noted in the VTA. (d–g) (e–g: higher magnification) Triple-labelling experiments showed that MOR-IR in the VTA was present on both dopaminergic and non-dopaminergic neurons projecting to the ACG. Some of MOR-labelled neurons that did not project to the ACG did not show TH-IR. (h) Percentages of MOR-, TH- and FG-labels, individually and in combination, in the VTA. Scale bars, 50 μm (a–d), 10 μm (e–g)

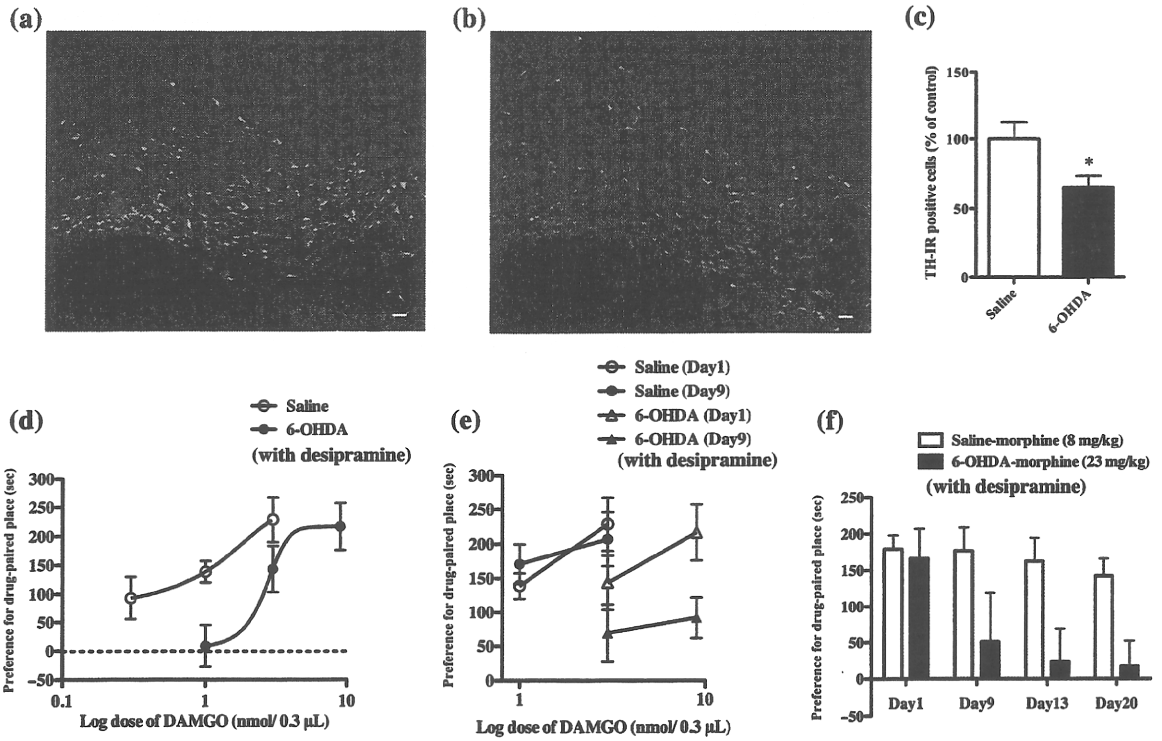

Figure 5 Involvement of dopamine neurons projecting from the VTA to the ACG in the DAMGO- or morphine-induced rewarding effect. (a–b) Colour photomicrographs of immunofluorescent staining of TH-IR cells in the rat VTA following saline (a) or 6-OHDA (b) injection into the ACG. (c) Percent of TH-IR positive cells in the VTA of rats showing the saline or 6-OHDA injection into the ACG. Student's *t*-test: $^{*}P < 0.05$ versus saline. (d) DAMGO-induced place preference in the saline-pre-treated and 6-OHDA-pre-treated groups using the CPP assay are shown. The ordinate shows the preference for the drug-paired place, as defined by the post-conditioning test score minus the pre-conditioning test score in the drug treatment side. Each point represents the mean conditioning score with SEM of 6–8 rats. (e) Extinction of the DAMGO-induced place preference. Data show the conditioned place preference scores in saline- or 6-OHDA-pre-treated groups of 6–8 rats. Conditioning was performed for six days after the pre-conditioning test. The post-conditioning test was performed on the day after the final conditioning test (one day). To investigate the extinction of the DAMGO-induced place preference, a post-conditioning test was performed at nine days after the final conditioning test. (f) Extinction of the morphine-induced place preference. Data show the conditioned place preference scores in saline- or 6-OHDA-pre-treated groups of six rats. To investigate the extinction of the morphine-induced place preference, a post-conditioning test was performed on 9, 13, 20 days after the final conditioning test. Scale bars, 50 μm (a–b)

selective D1 receptor antagonist SCH23390. Furthermore, the maintenance of morphine-induced place preference at 10 days after the final conditioning also was suppressed by pre-treatment of SCH23390 (Fig. 6a, b). The levels of phosphorylated-DARPP32 (Thr34) and phosphorylated-CREB (Ser133) in the ACG at 24 hours after the final conditioning were not affected by morphine (Fig. 6c, e), whereas the morphine-induced place preference at 10 days after the final conditioning produced significant increases of phosphorylated-DARPP32 (Thr34) and phosphorylated-CREB (Ser133) levels in the ACG. The increases of these levels in the ACG were blocked by pre-treatment of SCH23390 (Fig. 6d, f). Statistical analysis was performed with one-way ANOVA followed by Bonferroni's multiple comparison test ($^{*}P < 0.05$, $^{**}P < 0.01$ versus saline–saline, $\#P < 0.05$, $\#\#P < 0.01$ versus saline–morphine).

DISCUSSION

The mPFC is composed of the infralimbic (IL), prelimbic (PL) (area CG3 of the ACG), dorsal and ventral anterior cingulate (areas CG1 and CG2 of the ACG) and medial precentral (frontal area 1) cortical areas (Paxinos & Watson 1998; Ongur & Price 2000). The mPFC receives dopaminergic efferents from the VTA, and thus is part of the mesocortical dopamine system, with the densest innervation occurring within the IL and PL regions (Thierry *et al.* 1973; Conde *et al.* 1995). Within the mPFC, the PL is the main source of afferents to the IL. Other projections to the IL originate from the hippocampus (CA1/subiculum), basolateral amygdala (BLA) and VTA. The PL receives projections from the IL, CG1 and CG2, hippocampus (CA1/subiculum), BLA and VTA. The primary sources of afferents to the CG1 and CG2 are con-

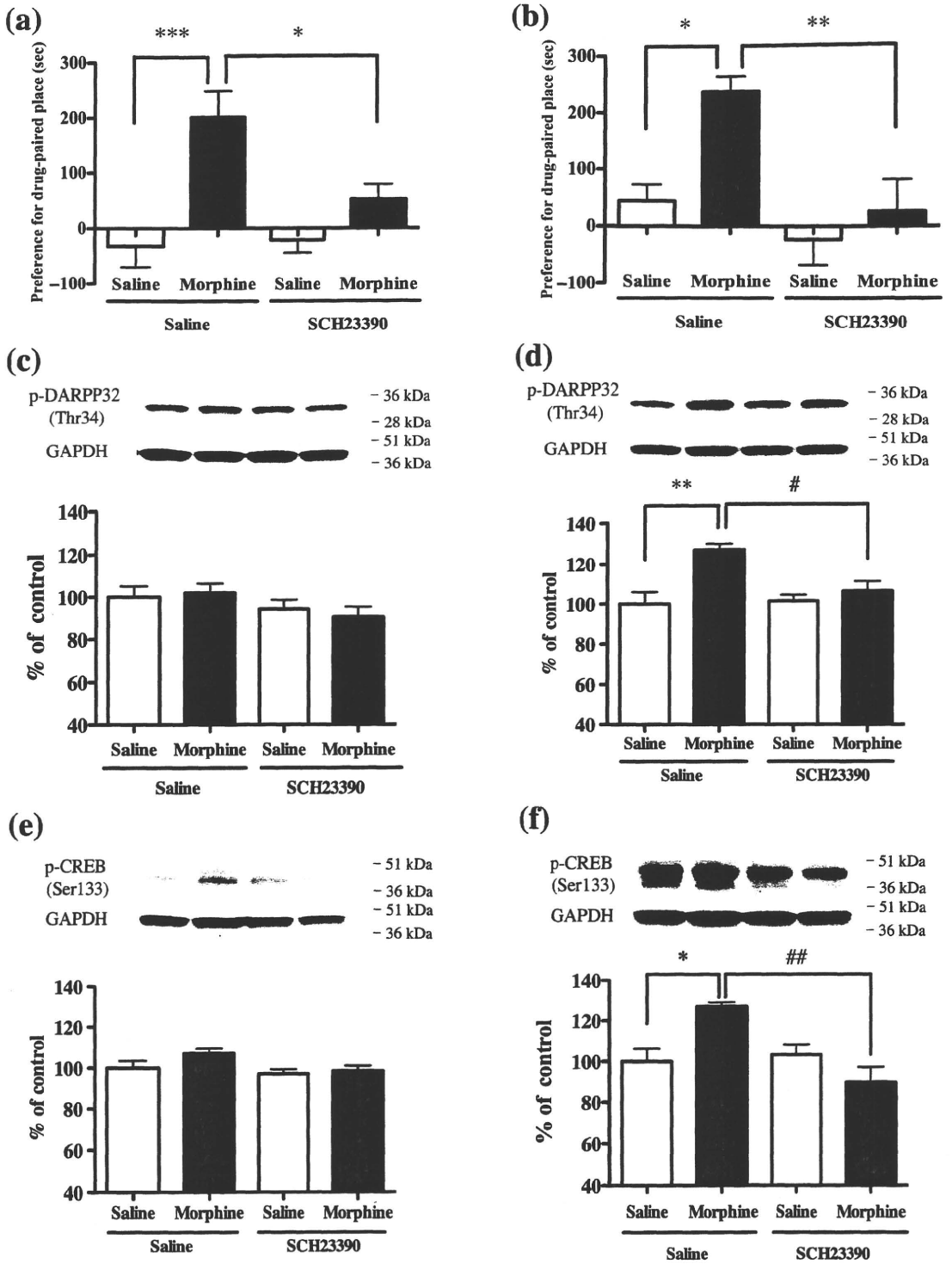

Figure 6 Changes in levels of phosphorylated DARPP32 (Thr34) or phosphorylated CREB (Ser133) in the ACG of rats that had acquired or maintained the morphine-induced place preference. (a–b) Change in the acquisition or maintenance of morphine-induced place preference at 24 hours (a) or 10 days (b) after the final conditioning. Data show the conditioned place preference scores in saline- or SCH23390-pre-treated saline or morphine groups of six rats. (c–d) Change in the level of phosphorylated DARPP32 (Thr34) in lysate fractions of the ACG at 24 hours (c) or 10 days (d) after the final conditioning. (e–f) Change in the level of phosphorylated CREB (Ser133) in lysate fractions of the ACG at 24 hours (e) or 10 days (f) after the final conditioning. In the conditioning session, the rats were administered morphine (8 mg/kg, i.p.) 15 minutes after the pre-treatment of saline or SCH23390 (0.1 mg/kg, i.p.). Each column represents the mean with SEM of at least three independent experiments. Bonferroni multiple comparison test: $*P<0.05$, $**P<0.01$ versus saline–saline, $\#P<0.05$, $\#\#P<0.01$ versus saline–morphine

sidered to be the PL, hippocampus (CA1/subiculum), BLA and VTA (Hoover & Vertes 2007). In the present study, several FG-positive VTA–ACG projecting neurons in the VTA showed a TH-positive reaction, which suggested the existence of dopamine transmission in the ACG projecting from the VTA in the rat. In contrast, some of them exhibited a TH-negative reaction, which is supported by the finding that some GABAergic neurons in the VTA project to the mPFC (Carr & Sesack 2000). Furthermore, by using the retrograde tracer CTb as well as FG, we found that neurons that project from the VTA to the ACG exist independently and do not branch off from VTA–N.Acc projecting neurons. Interestingly, the ACG projects to the dorsal striatum, whereas the IL and PL project to the shell and core of the N.Acc, respectively (Berendse, Galis-de Graaf & Groenewegen 1992). We found that pre-microinjection of 6-OHDA into the ACG failed to change the basal levels of dopamine and its metabolites in the N.Acc. To further verify the dopaminergic neurons that project directly from the VTA to the ACG, we investigated whether the VTA-ACG dopaminergic pathway could be activated by the electrical stimulation of VTA cells. As a result, dopamine release with increased levels of its metabolites at the synaptic terminal in the ACG was increased by the electrical stimulation of VTA cells. These results provide physiological evidence for the existence of VTA–ACG dopaminergic projection.

In both the paranigral and parabrachial nuclei, which are the two major VTA subdivisions, MOR-labelling was observed within somata and proximal dendrites and was sometimes continuous with labelled neuronal somata (Garzon & Pickel 2001). In the present study, MOR was found at a high density in the VTA and was detected in both dopaminergic and non-dopaminergic VTA neurons projecting to the ACG. Some of the MOR-labelled neurons with no projecting to the ACG were also non-dopaminergic. In addition, in a preliminary study, we found that some of the MOR-labelled non-dopaminergic neurons in the VTA were GABAergic neurons (data not shown). These results are supported by a report that MOR agonists in the VTA affect dopaminergic transmission mainly indirectly through changes in the postsynaptic responsivity and/or presynaptic release from neurons containing other neurotransmitters, whereas MOR agonists also directly affect a small population of dopaminergic neurons expressing MOR on their dendrites in the VTA (Garzon & Pickel 2001).

We next investigated the possible release of dopamine in the ACG by the intra-VTA administration of a MOR agonist. The dopamine level at the synaptic terminal in the ACG was markedly increased by microinjection of DAMGO into the VTA. Microinjection of DAMGO into the VTA also produced a significant increase in the dopamine metabolites DOPAC and HVA, indicating that activation of MORs in the VTA by intra-VTA microinjection of DAMGO activates the VTA–ACG dopaminergic pathway in a depolarization-dependent manner.

The CPP procedure has been used extensively as an animal model for investigating the rewarding properties of drug-conditioned stimuli. The CPP procedure has also been used to investigate inhibitory effects on the acquisition (Shoblock, Wichmann & Maidment 2005; Esmaeili *et al.* 2009), consolidation (Alberini 2008; Esmaeili *et al.* 2009), expression (Shoblock *et al.* 2005; Esmaeili *et al.* 2009), extinction (Shoblock *et al.* 2005; Zhai *et al.* 2008), reinstatement (Shoblock *et al.* 2005; Popik, Wrobel & Bisaga 2006; Zhai *et al.* 2008) and reconsolidation (Alberini 2008). In the present study, the DAMGO-induced place preference was attenuated by the pre-microinjection of 6-OHDA, which destroys dopaminergic neurons, into the ACG. This finding is supported by a report that kainic acid lesions of the ACG prevent the acquisition of a morphine-induced place preference in mice (Hao *et al.* 2008). It was also reported that quinolinic acid lesions of the IL blocked the CPP induced by morphine, while lesions of the PL did not affect a morphine-induced CPP (Tzschentke & Schmidt 1999). Taken together, these findings suggest that the IL, CG1 and CG2 areas in the mPFC may be involved in the acquisition of μ-opioid-induced CPP.

More interestingly, we found here for the first time that rats that had been subjected to the ACG-microinjection of 6-OHDA failed to maintain μ-opioid-induced place preference in the early phase. Furthermore, the levels of phosphorylated DARPP32 (Thr34) and phosphorylated CREB (Ser133) in the ACG were increased in rats that maintained the μ-opioid-induced place preference, whereas the increases of these levels were almost abolished by pre-treatment of a selective dopamine D1 receptor antagonist. Although further examinations are needed to identify the role of VTA–ACG dopaminergic neurons in learning and memory, the present findings provide evidence that D1/DARPP32/CREB pathway in the ACG may be critical for the maintenance of a place preference induced by μ-opioids.

In conclusion, we have demonstrated here that dopamine in the ACG can be released by the activation of MORs in the VTA by MOR agonists, and the dopaminergic transmission that projects from the VTA to the ACG may be crucial for the acquisition and maintenance of the rewarding effects of μ-opioids. Furthermore, the activation of D1/DARPP32/CREB signalling in the ACG may be involved in the maintenance of the μ-opioid-induced place preference.

Acknowledgements

This work was supported by a Grant-in-Aid for Scientific Research and a research grant from the Ministry of Edu-

cation, Culture, Sports, Science and Technology of Japan. We thank Dr Keisuke Hashimoto, Mr Yasuhisa Kobayashi, Ms Sayuri Ishiwata, Mr Masaharu Furuya and Mr Natsuki Honda for their expert technical assistance.

Authors Contribution

MN and YM designed the experiments and wrote the manuscript. YM was responsible for most of the experimental work. KN contributed some of retrograde tracing and biochemical studies. MN performed biochemical experiments. ST, KN, KK, MA and MS conducted some of *in vivo* studies. MA and SI contributed some of biochemical experiments. KI and NK provided scientific and technical advice. TS supervised the overall projects. All authors discussed the results and commented on the manuscript.

References

Alberini CM (2008) The role of protein synthesis during the labile phases of memory: revisiting the skepticism. Neurobiol Learn Mem 89:234–246.

Alhaider AA (1991) Antinociceptive effect of ketanserin in mice: involvement of supraspinal 5-HT2 receptors in nociceptive transmission. Brain Res 543:335–340.

Almarestani L, Warers SM, Krause JE, Bennett GJ, Ribeiro-da-Silva A (2007) Morphological characterization of spinal cord dorsal horn lamina I neurons projecting to the parabrachial nucleus in the rat. J Comp Neurol 504:287–297.

Berendse HW, Galis-de Graaf Y, Groenewegen HJ (1992) Topographical organization and relationship with ventral striatal compartments of prefrontal corticostriatal projections in the rat. J Comp Neurol 316:314–347.

Berger B, Gaspar P, Verney C (1991) Dopaminergic innervation of the cerebral cortex: unexpected differences between rodents and primates. Trends Neurosci 14:21–27.

Carr DB, Sesack SR (2000) GABA-containing neurons in the rat ventral tegmental area project to the prefrontal cortex. Synapse 38:114–123.

Conde F, Maire-Lepoivre E, Audinat E, Crepel F (1995) Afferent connections of the medial frontal cortex of the rat. II. Cortical and subcortical afferents. J Comp Neurol 352:567–593.

Damasio AR (1995) On some functions of the human prefrontal cortex. Ann N Y Acad Sci 769:241–251.

Esmaeili B, Basseda Z, Gholizadeh S, Javadi Paydar M, Dehpour AR (2009) Tamoxifen disrupts consolidation and retrieval of morphine-associated contextual memory in male mice: interaction with estradiol. Psychopharmacology 204: 191–201.

Garzon M, Pickel VM (2001) Plasmalemmal mu-opioid receptor distribution mainly in nondopaminergic neurons in the rat ventral tegmental area. Synapse 41:311–328.

Hao Y, Yang J, Sun J, Qi J, Dong Y, Wu CF (2008) Lesions of the medial prefrontal cortex prevent the acquisition but not reinstatement of morphine-induced conditioned place preference in mice. Neurosci Lett 433:48–53.

Hoover WB, Vertes RP (2007) Anatomical analysis of afferent projections to the medial prefrontal cortex in the rat. Brain Struct Funct 212:149–179.

Jentsch JD, Redmond DE Jr, Elsworth JD, Taylor JR, Youngren KD, Roth RH (1997a) Enduring cognitive deficits and cortical dopamine dysfunction in monkeys after long-term administration of phencyclidine. Science 277:953–955.

Jentsch JD, Tran A, Le D, Youngren KD, Roth RH (1997b) Subchronic phencyclidine administration reduces mesoprefrontal dopamine utilization and impairs prefrontal cortical-dependent cognition in the rat. Neuropsychopharmacology 17:92–99.

Kelley AE, Berridge KC (2002) The neuroscience of natural rewards: relevance to addictive drugs. J Neurosci 22:3306–3311.

Kishi T, Tsumori T, Yokota S, Yasui Y (2006) Topographical projection from the hippocampal formation to the amygdala: a combined anterograde and retrograde tracing study in the rat. J Comp Neurol 496:349–368.

Koob GF (1992) Drugs of abuse: anatomy, pharmacology and function of reward pathways. Trends Pharmacol Sci 13:177–184.

Laemmli UK (1970) Cleavage of structural proteins during the assembly of the head of bacteriophage T4. Nature 227:680–685.

Merriam EP, Thase ME, Haas GL, Keshavan MS, Sweeney JA (1999) Prefrontal cortical dysfunction in depression determined by Wisconsin Card Sorting Test performance. Am J Psychiatry 156:780–782.

Nestler EJ (2001) Molecular basis of long-term plasticity underlying addiction. Nat Rev Neurosci 2:119–128.

Ongur D, Price JL (2000) The organization of networks within the orbital and medial prefrontal cortex of rats, monkeys and humans. Cereb Cortex 10:206–219.

Paxinos G, Watson C (1998) The Rat Brain in Stereotaxic Coordinates, 4th edn. New York: Academic Press.

Peoples LL (2002) Neuroscience. Will, anterior cingulate cortex, and addiction. Science 296:1623–1624.

Pierce RC, Kumaresan V (2006) The mesolimbic dopamine system: the final common pathway for the reinforcing effect of drugs of abuse? Neurosci Biobehav Rev 30:215–238.

Popik P, Wrobel M, Bisaga A (2006) Reinstatement of morphine-conditioned reward is blocked by memantine. Neuropsychopharmacology 31:160–170.

Puumala T, Sirvio J (1998) Changes in activities of dopamine and serotonin systems in the frontal cortex underlie poor choice accuracy and impulsivity of rats in an attention task. Neuroscience 83:489–499.

Rushworth MF, Walton ME, Kennerley SW, Bannerman DM (2004) Action sets and decisions in the medial frontal cortex. Trends Cogn Sci 8:410–417.

Schweimer J, Saft S, Hauber W (2005) Involvement of catecholamine neurotransmission in the rat anterior cingulate in effort-related decision making. Behav Neurosci 119:1687–1692.

Shoblock JR, Wichmann J, Maidment NT (2005) The effect of a systemically active ORL-1 agonist, Ro 64-6198, on the acquisition, expression, extinction, and reinstatement of morphine conditioned place preference. Neuropharmacology 49:439–446.

Steen PA, Mason M, Pham L, Lefebvre Y, Hickmott PW (2007) Axonal bias at a representational border in adult rat somatosensory cortex (S1). J Comp Neurol 500:634–645.

Suzuki T, Masukawa Y, Misawa M (1990) Drug interactions in the reinforcing effects of over-the-counter cough syrups. Psychopharmacology 102:438–442.

Tallarida RJ, Porreca F, Cowan A (1989) Statistical analysis of drug–drug and site–site interactions with isobolograms. Life Sci 45:947–961.

Thierry AM, Blanc G, Sobel A, Stinus L, Golwinski J (1973) Dopaminergic terminals in the rat cortex. Science 182:499–501.

Tzschentke TM, Schmidt WJ (1999) Functional heterogeneity of the rat medial prefrontal cortex: effects of discrete subarea-specific lesions on drug-induced conditioned place preference and behavioural sensitization. Eur J Neurosci 11:4099–4109.

Tzschentke TM, Schmidt WJ (2000) Differential effects of discrete subarea-specific lesions of the rat medial prefrontal cortex on amphetamine- and cocaine-induced behavioural sensitization. Cereb Cortex 10:488–498.

Ventura R, Alcaro A, Puglisi-Allegra S (2005) Prefrontal cortical norepinephrine release is critical for morphine-induced reward, reinstatement and dopamine release in the nucleus accumbens. Cereb Cortex 15:1877–1886.

Walton ME, Bannerman DM, Alterescu K, Rushworth MF (2003) Functional specialization within medial frontal cortex of the anterior cingulate for evaluating effort-related decisions. J Neurosci 23:6475–6479.

Weinberger D (1995) Neurodevelopmental perspectives on schizophrenia. In: Bloom FE, Kupfer DJ, eds. The Fourth Generation of Progress, pp. 1171–1183. New York: Raven.

Williams GV, Goldman-Rakic PS (1995) Modulation of memory fields by dopamine D1 receptors in prefrontal cortex. Nature 376:572–575.

Wise SP, Murray EA, Gerfen CR (1996) The frontal cortex-basal ganglia system in primates. Crit Rev Neurobiol 10:317–356.

Zhai H, Wu P, Xu C, Liu Y, Lu L (2008) Blockade of cue- and drug-induced reinstatement of morphine-induced conditioned place preference with intermittent sucrose intake. Pharmacol Biochem Behav 90:404–408.

Neuropharmacology 58 (2010) 452–456

Contents lists available at ScienceDirect

Neuropharmacology

journal homepage: www.elsevier.com/locate/neuropharm

Serotonin 1A receptor gene is associated with Japanese methamphetamine-induced psychosis patients

Taro Kishi [a,*], Tomoko Tsunoka [a], Masashi Ikeda [a,b], Tsuyoshi Kitajima [a], Kunihiro Kawashima [a], Tomo Okochi [a], Takenori Okumura [a], Yoshio Yamanouchi [a], Yoko Kinoshita [a], Hiroshi Ujike [c,d], Toshiya Inada [c,e], Mitsuhiko Yamada [c,f], Naohisa Uchimura [c,g], Ichiro Sora [c,h], Masaomi Iyo [c,i], Norio Ozaki [c,j], Nakao Iwata [a,c]

[a] Department of Psychiatry, Fujita Health University School of Medicine, Toyoake, Aichi 470-1192, Japan
[b] Department of Psychological Medicine, School of Medicine, Cardiff University, Heath Park, Cardiff CF14 4XN, United Kingdom
[c] Japanese Genetics Initiative for Drug Abuse, Japan
[d] Department of Neuropsychiatry, Okayama University Graduate School of Medicine, Dentistry and Pharmaceutical Sciences, Okayama 700-8558, Japan
[e] Department of Psychiatry, Seiwa Hospital, Institute of Neuropsychiatry, Tokyo 162-0851, Japan
[f] National Institute of Mental Health, National Center of Neurology and Psychiatry, Ichikawa 272-0827, Japan
[g] Department of Neuropsychiatry, Kurume University School of Medicine, Kurume 830-0011, Japan
[h] Department of Psychobiology, Department of Neuroscience, Tohoku University Graduate School of Medicine, Sendai 980-8576, Japan
[i] Department of Psychiatry, Chiba University Graduate School of Medicine, Chiba 260-8677, Japan
[j] Department of Psychiatry, Nagoya University Graduate School of Medicine, Nagoya 466-8850, Japan

ARTICLE INFO

Article history:
Received 24 June 2009
Received in revised form
17 August 2009
Accepted 4 September 2009

Keywords:
Serotonin 1A receptor gene (*HTR1A*)
Functional SNP
Tagging SNP
Methamphetamine-induced psychosis

ABSTRACT

Background: Several investigations have reported associations the serotonin 1A (5-HT1A) receptor to schizophrenia and psychotic disorders, making 5-HT1A receptor gene (*HTR1A*) an adequate candidate gene for the pathophysiology of schizophrenia and methamphetamine (METH)-induced psychosis. Huang and colleagues reported that rs6295 in *HTR1A* was associated with schizophrenia. The symptoms of methamphetamine (METH)-induced psychosis are similar to those of paranoid type schizophrenia. It may indicate that METH-induced psychosis and schizophrenia have common susceptibility genes. In support of this hypothesis, we reported that the V-act murine thymoma viral oncogene homologue 1 (AKT1) gene was associated with METH-induced psychosis and schizophrenia in the Japanese population. Furthermore, we conducted an analysis of the association of *HTR1A* with METH-induced psychosis.

Method: Using one functional SNP (rs6295) and one tagging SNP (rs878567), we conducted a genetic association analysis of case-control samples (197 METH-induced psychosis patients and 337 controls) in the Japanese population. The age and sex of the control subjects did not differ from those of the methamphetamine dependence patients.

Results: Rs878567 was associated with METH-induced psychosis patients in the allele/genotype-wise analysis. Moreover, this significance remained after Bonferroni correction. In addition, we detected an association between rs6295 and rs878567 in *HTR1A* and METH-induced psychosis patients in the haplotype-wise analysis. Although we detected an association between rs6295 and METH-induced psychosis patients, this significance disappeared after Bonferroni correction.

Conclusion: HTR1A may play an important role in the pathophysiology of METH-induced psychosis in the Japanese population. However, because we did not perform a mutation scan of *HTR1A*, a replication study using a larger sample may be required for conclusive results.

1. Introduction

Altered serotonergic neural transmission is hypothesized to be a susceptibility factor for schizophrenia (Geyer and Vollenweider, 2008; Meltzer et al., 2003). Several postmortem studies reported increased serotonin 1A (5-HT1A) receptor in the prefrontal cortex

* Corresponding author. Tel.: +81 562 93 9250; fax: +81 562 93 1831.
E-mail address: tarok@fujita-hu.ac.jp (T. Kishi).

0028-3908/$ – see front matter
doi:10.1016/j.neuropharm.2009.09.006

of schizophrenic patients (Burnet et al., 1996; Hashimoto et al., 1993, 1991; Simpson et al., 1996; Sumiyoshi et al., 1996). Huang and colleagues reported that rs6295 in an SNP (C-1019G: rs6295) in the promoter region of the 5-HT1A receptor gene (*HTR1A*), which regulate HTR1A transcription (Le Francois et al., 2008; Lemonde et al., 2003), was associated with schizophrenia (Huang et al., 2004). These facts suggest a crucial relationship between the 5-HT1A receptor and schizophrenia, and that *HTR1A* is an adequate candidate for the etiology of schizophrenia. *HTR1A* (OMIM*109 760, 1 exon in this genomic region spanning 2.069 kb) is located on 5q11.

The symptoms of methamphetamine (METH)-induced psychosis are similar to those of paranoid type schizophrenia (Sato et al., 1992). It may indicate that METH-induced psychosis and schizophrenia have common susceptibility genes (Bousman et al., 2009). In support of this hypothesis, we reported that the V-act murine thymoma viral oncogene homologue 1 (AKT1) gene was associated with METH-induced psychosis (Ikeda et al., 2006) and schizophrenia (Ikeda et al., 2004) in the Japanese population. Furthermore, we conducted an analysis of the association of these genes with METH-induced psychosis, using the recently recommended strategy of 'gene-based' association analysis (Neale and Sham, 2004).

2. Materials and methods

2.1. Subjects

The subjects in the association analysis were 197 METH-induced psychosis patients (164 males: 83.2% and 33 females; mean age ± standard deviation (SD) 37.6 ± 12.2 years) and 337 healthy controls (271 males: 80.4% and 66 females; 37.6 ± 14.3 years). The age and sex of the control subjects did not differ from those of the methamphetamine dependence patients. All subjects were unrelated to each other, ethnically Japanese, and lived in the central area of Japan. The patients were diagnosed according to DSM-IV criteria with consensus of at least two experienced psychiatrists on the basis of unstructured interviews and a review of medical records. METH-induced psychosis patients were divided into two categories of psychosis prognosis, the transient type and the prolonged type, which showed remission of psychotic symptoms within 1 month and after more than 1 month, respectively, after the discontinuance of methamphetamine consumption and beginning of treatment with neuroleptics; 112 patients (56.9%) were the transient type, and 85 patients (43.1%) were the prolonged type. One hundred thirty-seven subjects with METH-induced psychosis also had dependence on drugs other than METH. Cannabinoids were the most frequency abused drugs (31.4%), followed by cocaine (9.09%), LSD (9.09%), opioids (7.69%), and hypnotics (7.69%). Subjects with METH-induced psychosis were excluded if they had a clinical diagnosis of psychotic disorder, mood disorder, anxiety disorder or eating disorder. More detailed characterizations of these subjects have been published elsewhere (Kishi et al., 2008b). All healthy controls were also psychiatrically screened based on unstructured interviews. None had severe medical complications such as liver cirrhosis, renal failure, heart failure or other Axis-I disorders according to DSM-IV.

The study was described to subjects and written informed consent was obtained from each. This study was approved by the Ethics Committee at Fujita Health University, Nagoya University School of Medicine and each participating member of the Institute of the Japanese Genetics Initiative for Drug Abuse (JGIDA).

2.2. SNPs selection and linkage disequilibrium (LD) evaluation

We first consulted the HapMap database (release#23.a.phase2, Mar 2008, www.hapmap.org, population: Japanese Tokyo: minor allele frequencies (MAFs) of more than 0.05) and included 3 SNPs (rs6449693, rs878567 and rs1423691) covering *HTR1A* (5′-flanking regions including about 1 kb from the initial exon and about 2 kb downstream (3′) from the last exon: HapMap database contig number chr5: 63287418...63291774). Then one tagging SNP was selected with the criteria of an r^2 threshold greater than 0.8 in 'pair-wise tagging only' mode using the 'Tagger' program (Paul de Bakker, http://www/broad.mit.edu/mpg/tagger) of the HAPLOVIEW software (Barrett et al., 2005).

HTR1A has also been reported to have one biologically functional SNP (C-1019G: rs6295) (Albert et al., 1996; Albert and Lemonde, 2004; Lemonde et al., 2003). Rs6295 (C-1019G) in the promoter region regulate *HTR1A* transcription (Le Francois et al., 2008; Lemonde et al., 2003). The C allele is a part of a 26 palindrome that connect transcription factors (Deaf-1, Hes1 and Hes5) by NUDR (nuclear deformed epidermal autoregulatory factor), whereas the G allele abolishes repression by NUDR (Le Francois et al., 2008; Lemonde et al., 2003). This would lead to elevated levels of 5-HT1A receptor in the presynaptic raphe nucleus in GG genotypes, compared with CC genotype (Le Francois et al., 2008; Lemonde et al., 2003). Since no information about rs6295 was shown in the HapMap database, we included this SNP. These two SNPs were then used for the following association analysis.

2.3. SNPs genotyping

We used TaqMan assays (Applied Biosystems, Inc., Foster City, CA) for both SNPs. Detailed information, including primer sequences and reaction conditions, is available on request.

2.4. Statistical analysis

Genotype deviation from the Hardy–Weinberg equilibrium (HWE) was evaluated by chi-square test (SAS/Genetics, release 8.2, SAS Japan Inc., Tokyo, Japan).

Marker-trait association analysis was used to evaluate allele- and genotype-wise association with the chi-square test (SAS/Genetics, release 8.2, SAS Japan Inc., Tokyo, Japan), and haplotype-wise association analysis was conducted with a likelihood ratio test using the COCAPHASE2.403 program (Dudbridge, 2003). We used the permutation test option as provided in the haplotype-wise analysis to avoid spurious results and correct for multiple testing. Permutation test correction was performed using 1000 iterations (random permutations). In addition, Bonferroni's correction was used to control inflation of the type I error rate in the single marker association analysis and in the explorative analysis. For Bonferroni correction, we employed the following numbers for multiple testing: 2 for each sample set in allele- and genotype-wise analysis (2 examined SNPs). We had already performed a permutation test in the haplotype-wise analysis. Power calculation was performed using a genetic power calculator (Purcell et al., 2003).

The significance level for all statistical tests was 0.05.

3. Results

The LD from rs6449693, rs878567 and rs1423691 was tight in from the HapMap database samples (r^2 = 1.00). However, the LD structure of rs6295 (functional SNP) and rs878567 (tagging SNP) in our control samples was not tight (r^2 = 0.160). Genotype frequencies of all SNPs were in HWE (Table 1). Rs878567 was associated with METH-induced psychosis patients in the allele/genotype-wise analysis (P allele = 0.000122 and P genotype = 0.00103) (Table 1). Moreover, these significances remained after Bonferroni correction (P allele = 0.000244 and P genotype = 0.00203) (Table 1). In addition, we detected an association between rs6295 and rs878567 in *HTR1A* and METH-induced psychosis patients in the haplotype-wise analysis (P = 0.0000643) (Table 2). Although we detected an association between rs6295 and METH-induced psychosis patients (P allele = 0.0271), this significance disappeared after Bonferroni correction (P allele = 0.0542) (Table 1).

4. Discussion

We found associations between *HTR1A* and Japanese METH-induced psychosis patients. Therefore, we reasoned that *HTR1A* may play an important role in the pathophysiology of METH-induced psychosis in the Japanese population. However, our samples are small. Although Bonferroni's correction was used to control inflation of the type I error rate, we considered that there is a possibility of type I error in these results.

The 5-HT1A receptor is present in various regions of the brain, including the cortex, hippocampus, amygdala, hypothalamus and septum (Aznar et al., 2003; Barnes and Sharp, 1999; Le Francois et al., 2008; Varnas et al., 2004). Presynaptic 5-HT1A autoreceptors play an important role in the autoregulation of serotonergic neurons (Le Francois et al., 2008; Lemonde et al., 2003; Riad et al., 2000; Sotelo et al., 1990). The 5-HT1A receptor activation by serotonin induces the hyperpolarization of serotonergic neurons, decreasing their firing rate and consequently the release of serotonin in the brain (Le Francois et al., 2008; Lemonde et al., 2003; Riad et al., 2000; Sotelo et al., 1990). Also, the 5-HT1A receptor was associated hippocampal neurogenesis. The hippocampus is a part of the limbic system involved in cognitive function such as memory. Stimulation of 5-HT1A receptors has been known to reduce the

Table 1
Association analysis of *HTR1A* with methamphetamine-induced psychosis.

SNP[a]	Phenotype[b]	MAFs[c]	N	Genotype distribution[d]			*P*-value[f]			Corrected *P*-value[f,g]	
				M/M	M/m	m/m	HWE[e]	Genotype	Allele	Genotype	Allele
rs6295	Controls	0.254	336	192	117	27	0.132				
C > G	METH-induced psychosis	0.317	197	92	85	20	0.955	0.0657	**0.0271**		0.0542
rs878567	Controls	0.126	336	258	71	7	0.423				
C > T	METH-induced psychosis	0.216	197	124	61	12	0.233	**0.00103**	**0.000122**	**0.00203**	**0.000244**

[a] Major allele > minor allele.
[b] METH-induced psychosis: methamphetamine-induced psychosis.
[c] MAFs: minor allele frequencies.
[d] M: major allele, m: minor allele.
[e] Hardy–Weinberg equilibrium.
[f] Bold represents significant *P*-value.
[g] Calculated using Bonferroni's correction.

negative symptoms and cognitive dysfunction of schizophrenia (Meltzer et al., 2003; Meltzer and Sumiyoshi, 2008; Sumiyoshi et al., 2001, 2007). Mason and Reynolds (1992) reported that one of the major pharmacological therapeutic targets of clozapine is 5-HT1A receptors on cortical glutamatergic neurons. Several post-mortem studies reported increased 5-HT1A receptor in the prefrontal cortex of schizophrenic patients (Burnet et al., 1996; Hashimoto et al., 1993, 1991; Simpson et al., 1996; Sumiyoshi et al., 1996). NAN-190 (5-HT1A receptor antagonist) produced an inhibitory action on methamphetamine-induced hyperactivity (Ginawi et al., 2004; Millan and Colpaert, 1991). These facts suggest that altered serotonergic neural transmission caused by abnormalities in 5-HT1A receptor may be involved in the development of psychotic disorders such as schizophrenia and METH-induced psychosis (Geyer and Vollenweider, 2008; Meltzer et al., 2003).

Serretti et al. (2007) reported that rs878567 in *HTR1A* was associated with German and Italian suicidal attempters. Also, previous study have reported that rs878567 in *HTR1A* was found the interaction with childhood physical abuse in mood disorders (Brezo et al., 2009). These authors suggested rs878567 might influence hippocampus-mediated memory deficits in mood disorders (Brezo et al., 2009). The LD from rs6449693, rs878567 and rs1423691 was tight in from the HapMap database samples (r^2 = 1.00). As these results show, rs878567 covers a wide and important region including the exon and the promoter region in *HTR1A*. Because it is possible that rs878567 influences biological function in the brain, we suggest that functional analysis for rs878567 should be performed in future studies.

Rs6295 (C-1019G) in the promoter region regulate *HTR1A* transcription (Le Francois et al., 2008; Lemonde et al., 2003). The C allele is a part of a 26 palindrome that connect transcription factors (Deaf-1, Hes1 and Hes5) by NUDR (nuclear deformed epidermal autoregulatory factor), whereas the G allele abolishes repression by NUDR (Le Francois et al., 2008; Lemonde et al., 2003). This would lead to elevated levels of 5-HT1A receptor in the presynaptic raphe nucleus in GG genotyps, compared with CC genotype (Le Francois et al., 2008; Lemonde et al., 2003). This variant was associated with several studies, including major depressive disorder (Anttila et al., 2007; Kraus et al., 2007; Lemonde et al., 2003; Neff et al., 2009; Parsey et al., 2006) and panic disorder (Strobel et al., 2003) and antidepressant response in MDD (Arias et al., 2005; Hong et al., 2006; Lemonde et al., 2004; Parsey et al., 2006; Serretti et al., 2004; Yu et al., 2006). Huang et al. (2004) reported that rs6295 was associated with schizophrenia. Recent studies reported that rs6295 was associated with the improvement in negative symptoms from antipsychotics such as risperidone (Mossner et al., 2009; Reynolds et al., 2006; Wang et al., 2008) and that 5-HT1A receptor agonists such as tandospirone produced improvements in the cognitive impairment in schizophrenia (Meltzer and Sumiyoshi, 2008; Sumiyoshi et al., 2001, 2007).

A few points of caution should be mentioned with respect to our results. Firstly, the positive association may be due to small sample size. Ideal samples for this study are METH use disorder samples with and without psychosis. Because we had only a few METH use disorder samples without psychosis, and we wanted to avoid statistical error, we did not perform an association analysis with these samples. Secondly, we did not include a mutation scan to detect rare variants. We designed the study based on the common disease-common variants hypothesis (Chakravarti, 1999). However, Weickert et al. (2008) have shown associations between a common disease such as schizophrenia and rare variants. If the genetic background of METH-induced psychosis is described by the common disease-rare variants hypothesis, further investigation will be required, such as medical resequencing using larger samples. However, statistical power is needed to evaluate the association of rare variants. Lastly, our subjects did not undergo structured interviews. However, in this study patients were carefully diagnosed according to DSM-IV criteria with consensus of at least two experienced psychiatrists on the basis of a review of medical records (Kishi et al., 2008a,c, 2009). In addition, when we found misdiagnosis in a patient, we promptly excluded the misdiagnosed case to maintain the precision of our sample. To overcome these limitations, a replication study using larger samples or samples of other populations will be required for conclusive results.

In conclusion, our results suggest that *HTR1A* may play a major role in the pathophysiology of METH-induced psychosis in the Japanese population. However, because we did not perform a mutation scan of *HTR1A*, a replication study using a larger sample may be required for conclusive results.

Table 2
Haplotype-wise analysis of *HTR1A*.

Haplotype rs6295-rs878567	Phenotype[a]	Individual haplotype frequency	Individual *P*-value[b]	Phenotype[a]	Global *P*-value[b]
C–C	Control	0.811			
	METH-induced psychosis	0.694	**0.0000364**	METH-induced psychosis	**0.0000643**
G–C	Control	0.189			
	METH-induced psychosis	0.306	**0.0000364**		

[a] METH-induced psychosis: methamphetamine-induced psychosis.
[b] Bold numbers represent significant *P*-value.